within double-layered membrane compartments. J. Biol. Chem. **278**:24388–24398.

59. **Wang, S. H., W. J. Syu, K. J. Huang, H. Y. Lei, C. W. Yao, C. C. King, and S. T. Hu.** 2002. Intracellular localization and determination of a nuclear localization signal of the core protein of dengue virus. J. Gen. Virol. **83**: 3093–3102.
60. **Wang, Y., M. Lobigs, E. Lee, and A. Mullbacher.** 2003. $CD8^+$ T cells mediate recovery and immunopathology in West Nile virus encephalitis. J. Virol. **77**: 13323–13334.
61. **Westaway, E. G., A. A. Khromykh, M. T. Kenney, J. M. Mackenzie, and M. K. Jones.** 1997. Proteins C and NS4B of the flavivirus Kunjin translocate independently into the nucleus. Virology **234**:31–41.
62. **Wurm, T., H. Chen, T. Hodgson, P. Britton, G. Brooks, and J. A. Hiscox.** 2001. Localization to the nucleolus is a common feature of coronavirus nucleoproteins, and the protein may disrupt host cell division. J. Virol. **75**: 9345–9356.
63. **Yamshchikov, V. F., and R. W. Compans.** 1994. Processing of the intracellular form of the West Nile virus capsid protein by the viral NS2B-NS3 protease: an in vitro study. J. Virol. **68**:5765–5771.
64. **Yang, K. D., W. T. Yeh, R. F. Chen, H. L. Chuon, H. P. Tsai, C. W. Yao, and M. F. Shaio.** 2004. A model to study neurotropism and persistency of Japanese encephalitis virus infection in human neuroblastoma cells and leukocytes. J. Gen. Virol. **85**:635–642.

JOURNAL OF VIROLOGY, Jan. 2005, p. 1271–1281
0022-538X/05/$08.00+0 doi:10.1128/JVI.79.2.1271–1281.2005

Vol. 79, No. 2

# Molecular Determinants for Subcellular Localization of Hepatitis C Virus Core Protein

Ryosuke Suzuki,[1] Shinichiro Sakamoto,[1] Takeya Tsutsumi,[1] Akiko Rikimaru,[1,2] Keiko Tanaka,[3] Takashi Shimoike,[1] Kohji Moriishi,[4] Takuya Iwasaki,[3,5] Kiyohisa Mizumoto,[2] Yoshiharu Matsuura,[4] Tatsuo Miyamura,[1] and Tetsuro Suzuki[1]*

*Department of Virology II, National Institute of Infectious Diseases, Shinjuku-ku,[1] Department of Biochemistry, School of Pharmaceutical Sciences, Kitasato University, Minato-ku,[2] and Department of Pathology, National Institute of Infectious Diseases, Shinjuku-ku,[3] Tokyo, Research Center for Emerging Infectious Diseases, Research Institute for Microbial Diseases, Osaka University, Suita-shi, Osaka,[4] and Department of Pathology, Institute of Tropical Medicine, Nagasaki University, Nagasaki-shi, Nagasaki,[5] Japan*

Received 21 June 2004/Accepted 26 July 2004

**Hepatitis C virus (HCV) core protein is a putative nucleocapsid protein with a number of regulatory functions. In tissue culture cells, HCV core protein is mainly located at the endoplasmic reticulum as well as mitochondria and lipid droplets within the cytoplasm. However, it is also detected in the nucleus in some cells. To elucidate the mechanisms by which cellular trafficking of the protein is controlled, we performed subcellular fractionation experiments and used confocal microscopy to examine the distribution of heterologously expressed fusion proteins involving various deletions and point mutations of the HCV core combined with green fluorescent proteins. We demonstrated that a region spanning amino acids 112 to 152 can mediate association of the core protein not only with the ER but also with the mitochondrial outer membrane. This region contains an 18-amino-acid motif which is predicted to form an amphipathic α-helix structure. With regard to the nuclear targeting of the core protein, we identified a novel bipartite nuclear localization signal, which requires two out of three basic-residue clusters for efficient nuclear translocation, possibly by occupying binding sites on importin-α. Differences in the cellular trafficking of HCV core protein, achieved and maintained by multiple targeting functions as mentioned above, may in part regulate the diverse range of biological roles of the core protein.**

Hepatitis C virus (HCV), the most important causative agent of posttransfusion and sporadic non-A, non-B hepatitis, is a positive-stranded RNA virus belonging to the family *Flaviviridae* (7). A precursor polyprotein of about 3,000 amino acids is encoded by a large open reading frame of the genome and undergoes cellular and viral protease-mediated posttranslational modification to produce a series of structural and nonstructural proteins (8, 13, 16).

HCV core protein, which is derived from the N terminus of the viral polyprotein, forms multimers and interacts physically with the viral RNA to constitute the nucleocapsid (28, 47, 50). Tissue transglutaminase is responsible for stabilizing the core protein by cross-linking it into a dimeric form (26). In addition, the core viral protein has properties which enable it to modulate a number of cellular processes, including transcription, inhibition or stimulation of apoptosis, and suppression of host immunity, as reviewed previously (21, 29, 51, 52). Several studies suggest that expression of the core protein affects mitochondrial function and lipid metabolism. The core protein increases the cellular production of reactive oxygen species with subsequent increases in lipid peroxidation (35, 39). The viral protein also colocalizes with human apolipoprotein AII, associates with lipid droplets, and has the capacity to influence metabolic events involving lipid storage (2, 17, 30, 36, 44). In addition, the core protein reduces microsomal triglyceride transfer, leading to defects in very low density lipoprotein assembly and secretion (40). Furthermore, the HCV core protein has transforming potential in some cells under certain conditions (5, 42). Transgenic mice expressing this protein in the liver develop hepatic steatosis due to increased oxidative stress in the absence of inflammation, with subsequent development of hepatocellular carcinoma (34, 36). These results suggest that the HCV core protein might play a pivotal role in the pathogenesis of hepatitis C in addition to its role as a structural component of the viral capsid.

The amino acid sequence of the core protein is well conserved among different HCV isolates and genotypes compared to other HCV proteins. The N-terminal domain of the HCV core protein is highly basic, while its C terminus is hydrophobic. Although several core proteins of various sizes exist (17 to 23 kDa) (15, 23, 25, 49, 56), two processing events result in the predominant production of a 21-kDa core protein. Both of these events utilize the endoplasmic reticulum (ER). The first one is to be cleaved from downstream envelope protein E1 at position 191, where the C-terminal hydrophobic domain serves as a putative signal peptide sequence. Subsequently, the signal sequence of 13 or 18 residues is processed by signal peptide peptidase (19, 23, 56).

The HCV core protein is found primarily within the membranes of cytoplasmic organelles, but it is also found in the nucleus (23, 48, 56). Immunofluorescence studies show a punc-

* Corresponding author. Mailing address: Department of Virology II, National Institute of Infectious Diseases, 1-23-1 Toyama, Shinjuku-ku, Tokyo, Japan 162-8640. Phone: (81) 3-5285-1111. Fax: (81) 3-5285-1161. E-mail: tesuzuki@nih.go.jp.

tate pattern, consistent with ER localization, as well as perinuclear localization (15, 24, 32, 46, 56). Some studies suggest direct effects of the core protein on mitochondrial function. In fact, the core protein localizes to the mitochondria (34, 39). The N-terminal domain of the core protein contains three stretches of arginine- and lysine-rich sequences. Translocation of the core protein to the nucleus, mediated by these basic-residue stretches which function as nuclear localization signals (NLSs), is observed (6, 48). In addition, Moriishi et al. demonstrated that the N-terminal region of the core protein is also essential for nuclear retention through its interaction with the proteasome activator PA28γ (33).

In this study, we found a region that is important for localization of the mature core protein to the ER and to the mitochondrial outer membrane. We also identified a novel bipartite NLS responsible for nuclear targeting of the core protein, presumably via an importin-dependent pathway.

## MATERIALS AND METHODS

**Plasmid construction.** The construction of a plasmid expressing the full-length core protein of 191 amino acids, pCAGC191, was described previously (49). pGFP, a construct expressing green fluorescent protein (GFP) with a C-terminal Myc epitope tag sequences, was prepared as follows. pCMV/Myc/mito/GFP (Invitrogen Corp., Carlsbad, Calif.) was digested with PmlI, followed by treatment with the Klenow fragment of DNA polymerase I. The resultant linear fragment was ligated to a PstI linker (GCTGCAGC) and digested with PstI to remove the mitochondrial targeting signal sequence, followed by self-ligation. A series of HCV core-GFP fusion constructs were made by amplifying the core gene fragments with PCR with primers containing Flag epitope tag sequences (sense) and a PstI site (both). After digestion with PstI, the segments were inserted into the PstI site of pGFP. A series of GFP-core-E1 fusion constructs were made by amplifying core and E1 gene fragments with PCR with primers containing a NotI site. After digestion with NotI, the segments were inserted into the NotI site of pGFP.

pGEX-4T-1 (Amersham Bioscience Corp., Piscataway, N.J.) was used to express core protein fused with glutathione *S*-transferase (GST) in *Escherichia coli*. Core cDNA fragments encoding amino acids 1 to 71 were inserted into the EcoRI site of pGEX-4T-1. Alanine substitutions were introduced into the core protein by PCR mutagenesis with primers containing base alterations. The PCR products were then cloned into pCR2.1 (Invitrogen Corp.) and verified by DNA sequencing. Individual cDNAs were excised and inserted separately into pGFP or pGEX-4T-1. The primer sequences used in this study are available from the authors upon request.

Plasmid pRSET-hSRP1α (54), containing importin-α cDNA under the control of a T7 promoter, was kindly provided by Karsten Weis (University of California, Berkeley). A cDNA clone of importin-α possessing 14 residues (MYPYDVP DYGGGGS), derived in part from the hemagglutinin (HA) tag at the N terminus, was constructed by PCR. The resultant linear fragment was inserted under the control of a CAG promoter of pCAGGS and designated pCAG-HA-imp.

**Cell culture and transfection.** Human embryonic kidney 293T cells were maintained in Dulbecco's modified Eagle's medium supplemented with 100 units of penicillin per ml, 100 μg of streptomycin per ml, and 10% fetal bovine serum at 37°C in a 5% $CO_2$ incubator. Monolayers of 293T cells were transfected with plasmid DNA in the presence of Lipofectamine (Gibco-BRL, Life Technologies, Gaithersburg, Md.) according to the manufacturer's instructions.

**Confocal immunofluorescence microscopy.** Transfected cells were grown on glass coverslips. Two days after transfection, cells were fixed with 4% paraformaldehyde in phosphate-buffered saline (PBS) for 20 min at room temperature. Intracellular localization of HCV core-GFP fusion proteins was visualized in cells transfected with a variety of GFP fusion constructs.

In order to detect the HCV core protein by immunofluorescence, fixed cells were permeabilized with 0.2% Triton X-100 in PBS for 3 min at room temperature, followed by blocking with a nonfat milk solution (Block Ace; Snow Brand Milk Products Co., Sapporo, Japan). The cells were then incubated with anticore monoclonal antibody B2 (Anogen, Mississauga, Canada) for 60 min at room temperature, followed by incubation with fluorescein isothiocyanate-conjugated rabbit anti-mouse immunoglobulin G (IgG) (ICN Pharmaceuticals, Aurora, Ohio) for 45 min. To visualize mitochondria, MitoTracker Red CM-$H_2$XRos (Molecular Probes, Eugene, Oreg.) was added to the culture medium to a final concentration of 100 nM and incubated for 120 min at 37°C prior to fixation. To visualize the ER, goat anticalregulin antibody (Santa Cruz Biotechnology, Santa Cruz, Calif.) and rhodamine-conjugated rabbit anti-goat IgG (ICN Pharmaceuticals) were used as the first and second antibodies, respectively. To visualize HA-importin-α, mouse anti-HA antibody (Roche Molecular Biochemicals, Indianapolis, Ind.) and rhodamine-conjugated goat anti-mouse IgG (ICN Pharmaceuticals) were used as the first and second antibodies, respectively. All specimens were examined with an LSM510 laser scanning confocal microscope (Carl Zeiss, Oberkochen, Germany).

**Immunoelectron microscopy.** Cells were transfected as described above. After 2 days, cells were fixed with 3% paraformaldehyde and 0.1% glutaraldehyde in 0.1 M PBS (pH 7.4). Free aldehyde groups were quenched with 50 mM $NH_4Cl$ in PBS. The cell pellets were embedded at progressively lower temperatures (down to −35°C) in Lowicryl k4M according to an established protocol (43). Ultrathin sections were prepared and mounted on carbon-coated nickel grids. To perform electron microscopy, Lowicryl k4M ultrathin sections, mounted on grids, were floated on a droplet of PBS containing 1% bovine serum albumin, 0.1% Triton X-100, and 0.1% Tween 20 for 10 min, after which they were exposed to droplets of mouse anticore monoclonal antibody (Anogen) diluted in PBS for 45 min. Following this, they were rinsed twice for 5 min each in PBS and incubated with anti-mouse IgG-coated 10-nm immunogold particles (British Biocell, Cardiff, United Kingdom) for 45 min. After rinsing with PBS and distilled water, the grids and embedded sections were air dried and exposed to uranyl and lead acetate contrast agents.

**Subcellular fractionation.** All steps were performed at 4°C in the presence of a protease inhibitor cocktail called Complete (Roche Molecular Biochemicals). To isolate the ER fraction, transfected cells were washed with PBS, lysed in homogenization buffer A (50 mM Tris-HCl [pH 8.0], 1 mM β-mercaptoethanol, 1 mM EDTA, and 0.32 M sucrose), and then centrifuged at 5,000 × *g* for 10 min. The supernatant was then collected and centrifuged at 105,000 × *g* for 1 h. The pellet was disrupted in lysis buffer (50 mM Tris-HCl [pH 7.5], 150 mM NaCl, 1% NP-40, 1 mM dithiothreitol, 1 mM sodium orthovanadate, and 10 mM sodium fluoride), after which it was centrifuged at 15,000 × *g* for 20 min. The resulting supernatant was used as the ER fraction.

To isolate the mitochondrial fraction, transfected cells were washed with PBS and homogenized in ice-cold homogenization buffer B (200 mM mannitol, 50 mM sucrose, 1 mM EDTA, and 10 mM Tris-HCl) at pH 7.4. The supernatant was then centrifuged at 1,000 × *g* for 10 min to remove large debris and nuclei. The resulting supernatant was then centrifuged at 20,000 × *g* for 20 min to obtain crude mitochondria. The crude mitochondria pellet was subfractionated in Nycodenz gradients for further purification of mitochondria. Nycodenz (Axis-Shield PoC AS, Oslo, Norway) solution at 50% (wt/vol) was prepared in buffer containing 5 mM Tris-HCl and 1 mM EDTA at pH 7.4. This stock solution was then diluted with buffer containing 0.25 M sucrose, 5 mM Tris-HCl, and 1 mM EDTA at pH 7.4 before use. The crude mitochondrial pellets was suspended in 4 ml of 25% Nycodenz solution and overlaid onto the following discontinuous Nycodenz gradients: 1 ml of 40%, 1 ml of 34%, and 2 ml of 30%. The samples were topped off with 2 ml of 23% Nycodenz solution after placement onto the discontinuous gradients. The tubes were then centrifuged at 52,000 × *g* for 90 min. The dense band seen after centrifugation at the 25 to 30% interface was recovered as the purified mitochondrial fraction.

To determine the submitochondrial localization pattern of the core protein, mitochondria were resuspended in SH buffer (0.6 M sorbitol and 20 mM HEPES-KOH [pH 7.2]) in the absence or presence of 30 μg of proteinase K per ml after purification by Nycodenz density gradient centrifugation. Samples were incubated for 30 min at 0°C, after which protease digestion was halted by the addition of *p*-aminophenyl methanesulfonyl fluoride hydrochloride (*p*-APMSF) (5 mM). Proteins lysed in sodium dodecyl sulfate (SDS) sample buffer were analyzed by SDS-polyacrylamide gel electrophoresis (PAGE) and immunoblotted as described below.

**Immunoblot analysis.** The proteins were transferred to a polyvinylidene difluoride membrane (Immobilon; Millipore, Tokyo, Japan) after separation by SDS-PAGE. After blocking, the membranes were probed with monoclonal- or polyclonal-antibody against core protein (Anogen), prohibitin (Neo Markers, Fremont, Calif.), ribophorin I (Santa Cruz Biotechnology), translocase of the outer membrane (Tom) 20 (Santa Cruz Biotechnology), translocase of the inner membrane (Tim) 17 (Santa Cruz Biotechnology), or GFP (Santa Cruz Biotechnology). Immunoblots were developed as previously described (15).

**GST pulldown assay.** *Escherichia coli* BL21 cells were transformed with GST-core fusion plasmids and grown at 37°C. Expression of the fusion protein was induced by 1 mM isopropyl-β-D-thiogalactopyranoside at 37°C for 3 h. Bacteria were harvested, suspended in lysis buffer (1% Triton X-100 in PBS), and soni-

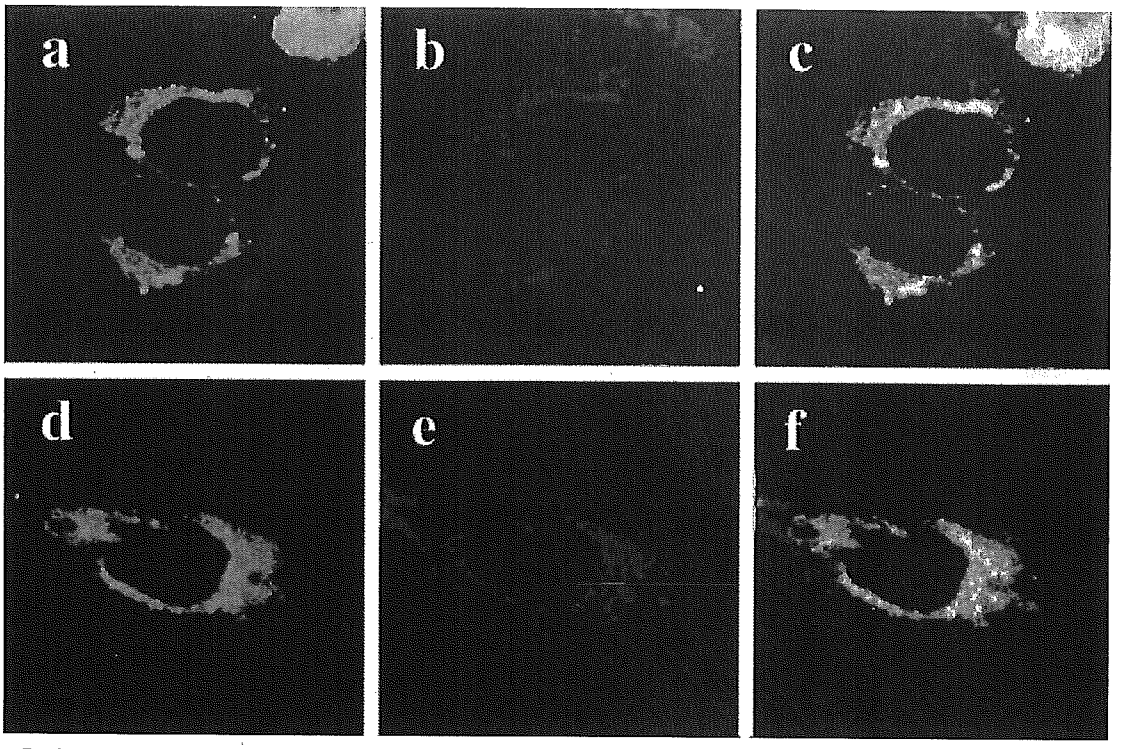


FIG. 1. Confocal analysis of double staining for HCV core protein and ER or mitochondria. 293T cells transfected with full-length HCV core expression plasmid, pCAGC191 were allowed to express the plasmid for 2 days. Transfected cells were fixed directly (a to c) or fixed after loading with Mitotracker (d to f). After permeabilization with Triton X-100, cells were subjected to immunofluorescence staining with a mouse anticore antibody. A goat anticalregulin antibody was used for ER staining. The green signals corresponding to the core were found with a fluorescein isothiocyanate-conjugated rabbit anti-mouse IgG (a and d). The red signals corresponding to the ER were obtained with a rhodamine-conjugated rabbit anti-goat IgG secondary antibody (b). Mitochondria were stained with the mitochondrion-selective dye Mitotracker (e). Overlay resulted in yellow signals indicative of colocalization (c and f).

cated on ice. GST and GST fusion proteins were purified from bacterial lysates with glutathione-Sepharose beads (Amersham Bioscience Corp.). The beads were washed four times with lysis buffer. Approximately equal amounts of purified protein, as estimated by Coomassie brilliant blue staining, were used for the binding assays. For pulldown assays, in vitro transcription and translation of importin-α was done with pRSET-hSRP1α and the TNT-coupled reticulocyte lysate system (Promega Corp., Madison, Wis.) with T7 RNA polymerase. The reaction was carried out at 30°C for 4 h in the presence of [$^{35}$S]methionine/cysteine (ICN Pharmaceuticals). The translation product was then incubated with glutathione-Sepharose beads bound to GST fusion proteins in 1 ml of binding buffer (40 mM HEPES [pH 7.5], 100 mM KCl, 0.1% NP-40, and 20 mM 2-mercaptoethanol) at 4°C for 1 h. The beads were washed four times with binding buffer, and the pulldown complexes were separated by SDS-PAGE on 15% polyacrylamide gels. The gels were then fixed, dried, and analyzed with autoradiography.

## RESULTS

**Subcellular localization of HCV core protein.** To assess the subcellular localization of HCV core protein, we first analyzed cells transfected with a full-length core-expressing construct by confocal microscopy. In accordance with previous observations (2, 15, 32, 45, 56), a granular cytoplasmic staining pattern of the core protein was observed in 293T (Fig. 1) and human hepatoblastoma HepG2 (data not shown) cells. Dual staining of transfected cells with antibody against the ER protein calregulin along with anticore antibody confirmed the ER localization of the core protein (Fig. 1a, b, and c show the core,

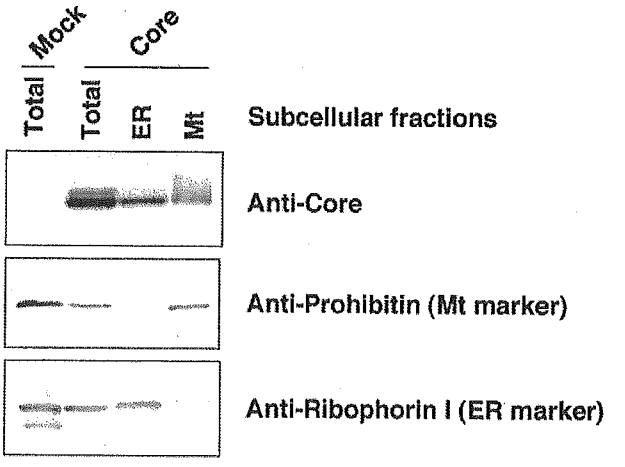


FIG. 2. Subcellular distribution of HCV core protein analyzed by immunoblotting. ER and mitochondrial (Mt) fractions were isolated from 293T cells expressing the full-length core protein (Core) or nontransfected cells (Mock) 2 days after transfection. Equal amounts of protein from each fraction as well as whole cell lysates (Total) were subjected to immunoblotting with a monoclonal antibody against either HCV core, prohibitin, or ribophorin I.

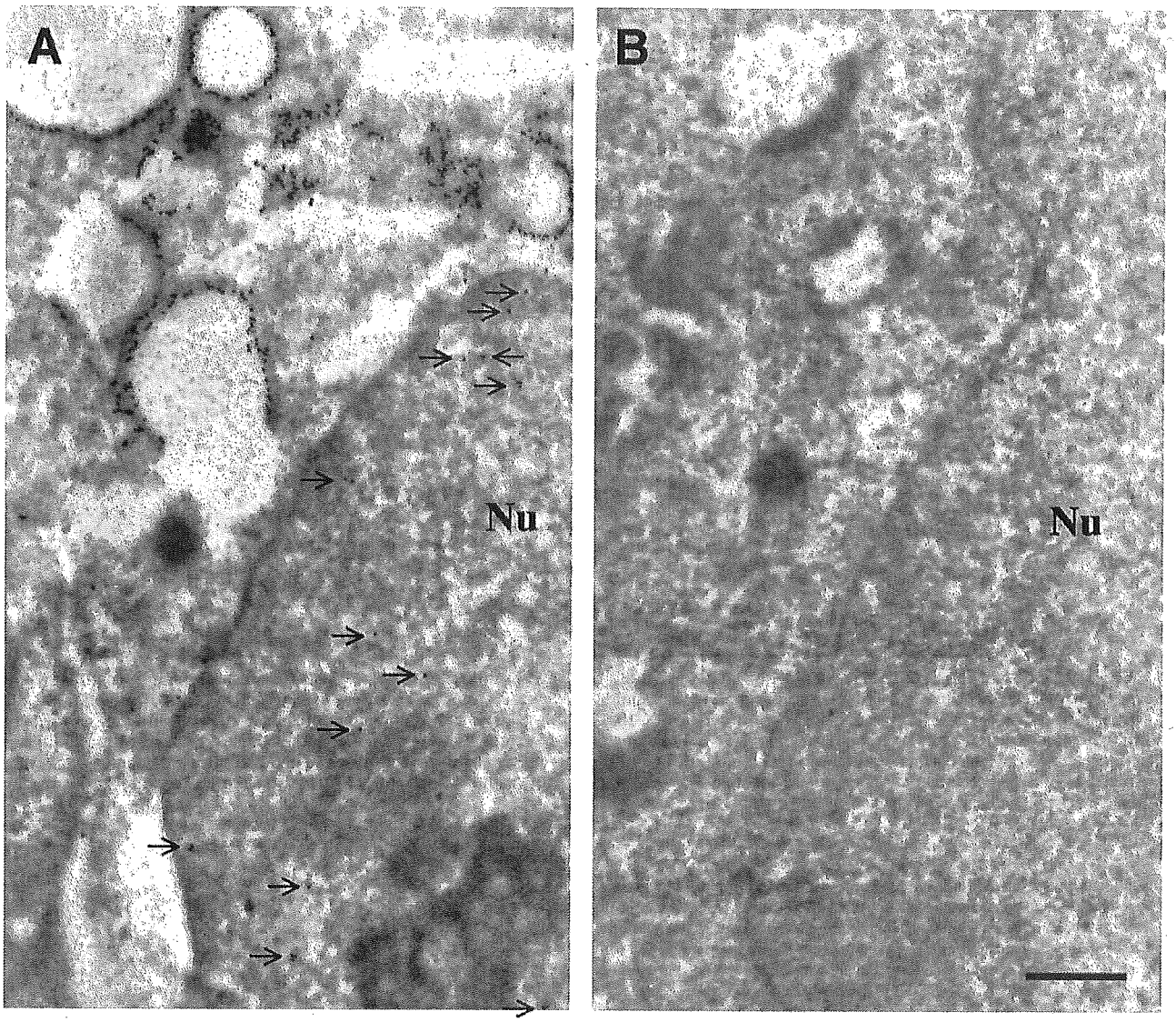


FIG. 3. Immunoelectron microscopy of HCV core protein. 293T cells expressing the full-length core protein (A) and nonexpressing cells (B) fixed 2 days after transfection. Immunoelectron microscopic analysis was performed with a mouse anticore antibody and a secondary anti-mouse IgG conjugated with gold particles. The arrows indicate the core protein localized in the nucleus (Nu). Bar, 500 nm.

calregulin, and a merged image, respectively). The pattern of subcellular localization of the core protein (Fig. 1d) was compared to the distribution of mitochondria, as revealed by MitoTracker staining (Fig. 1e). Although distribution of the core protein was not completely identical with that of the mitochondrion-selective dye, overlapping staining was observed, particularly in the perinuclear region (Fig. 1f).

Intracellular localization of the core protein was further examined in 293T cells by subcellular fractionation and Western blotting. The core protein was present in both the ER and mitochondrial fractions (Fig. 2), while it was not detected in the cytosol fraction (data not shown). The purity of the ER and mitochondrial fractions was confirmed with antibodies against ribophorin I as an ER marker and prohibitin as a mitochondrial marker.

It is generally difficult to identify the nuclear distribution of proteins of interest due to contamination of the nuclear preparation with unbroken, intact cells. Thus, to investigate whether the core protein localizes to the nucleus, we examined transfected cells by immunoelectron microscopy. Although gold particles were primarily observed within cytoplasmic membranes, perhaps highlighting the ER, immunoreactivity to anticore antibody was also observed in the nucleus (Fig. 3A, arrows). In contrast, no antibody labeling was observed in cells transfected with an empty vector (Fig. 3B).

Thus, HCV core protein predominates in the cytoplasm in a membrane-associated form(s) with ER and mitochondria, but nuclear localization is also observed.

**Regions responsible for directing core protein to the ER and mitochondria.** Given the tendency of the core protein to lo-

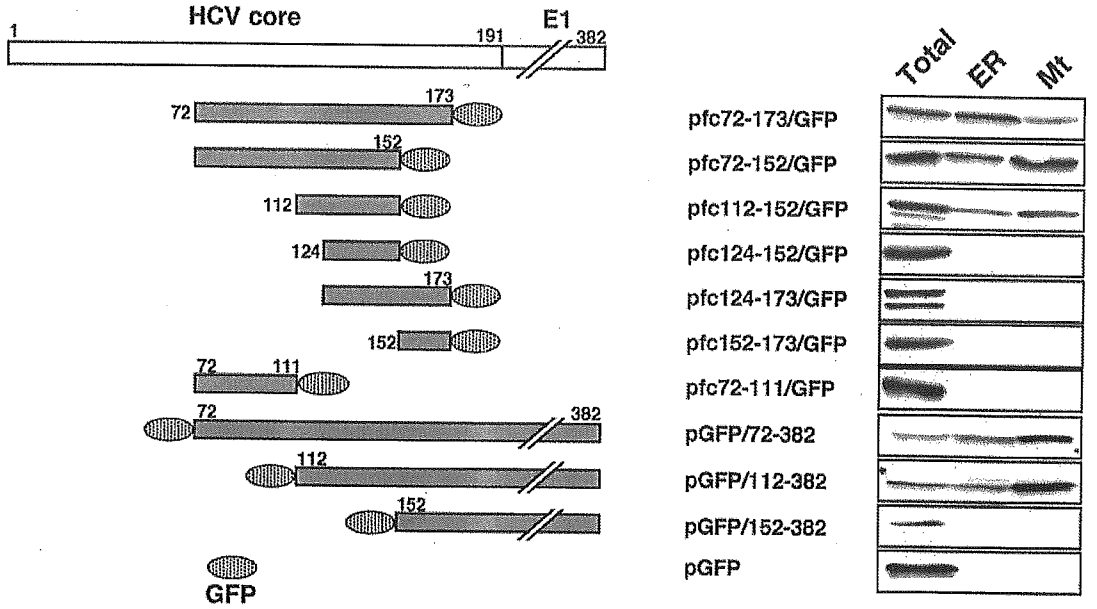


FIG. 4. Identification of segments that mediate association with ER and mitochondria in the core protein. Schematic diagram (left) and nomenclature (middle) of the core-GFP fusions are shown. Gray bars, expressed core and E1 regions. Subcellular distribution of fusion proteins is indicated on the right. ER and mitochondrial (Mt) fractions as well as whole-cell lysates (Total) were subjected to immunoblotting with an anti-GFP antibody.

calize to the ER and to mitochondria, we next investigated whether specific sequences might be responsible for transporting the core protein to these organelles. Fusion proteins between different regions of the core protein and GFP were developed, with specific emphasis on the region downstream of amino acid 72 because this region contains clusters of hydrophobic amino acids and the N-terminal 71 residues of the core are known to play a role in nuclear targeting (6, 48).

Western blotting of subcellular fractions with anti-GFP antibody revealed the localization of a core (72–173)-GFP fusion protein to the ER and to mitochondria (Fig. 4). Fusion proteins containing GFP and core proteins with N- or C-terminal deletions (72-152-GFP and 112-152-GFP) were likewise identified within the ER and mitochondrial fractions. In contrast, the ER and mitochondrial fractions did not contain GFP fusion proteins containing core protein amino acids 124 to 152, 124 to 173, 152 to 173, or 72 to 111. These fusion proteins demonstrated distribution profiles similar to that of GFP alone. We also tested GFP-core-E1 fusions, which are processed at the C terminus of the core by signal peptidase and signal peptide peptidase (19, 30). GFP-core fusions expressed from pGFP/72–382 and pGFP/112–382 were detected in the ER and mitochondrial fractions. The fusion expressed from pGFP/152–382 was not identified in these fractions.

We further analyzed subcellular localization of the fusion proteins by confocal immunofluorescence microscopy (Fig. 5). As expected, fusions of (72–173)-GFP and (112–152)-GFP exhibited localization to the ER and mitochondria. The patterns of subcellular localization of these fusions are indistinguishable from that of the full-length core protein, as shown in Fig. 1. Expression of (124–152)-GFP or (112–123)-GFP resulted in widespread diffusion of the fusion in the cell. Thus, these results indicate that the region spanning amino acids 112 to 152 can mediate association of the core protein not only to the ER but also to the mitochondria.

We subsequently examined the submitochondrial localization of the core protein with a protease protection assay. As shown in Fig. 6A, HCV core protein localized in the mitochondria was completely digested upon treatment with proteinase K for 30 min at 0°C. Under identical conditions, a marker specific for the mitochondrial outer membrane, Tom20, was also observed to disappear, whereas digestion of a mitochondrial inner membrane marker, Tim17, was not observed. These findings confirm that HCV core protein is localized to the mitochondrial outer membrane.

The predicted secondary structure of the region, amino acids 72 to 173, is shown in Fig. 6B. The presence of a long helical segment, lying between amino acids 116 and 134, and two short α-helices (amino acids 146 to 152 and amino acids 155 to 159) were predicted. The results of the cell fractionation assay and confocal microscopy with a series of deletion mutants shown in Fig. 4 and 5 suggest that an α-helix between amino acids 116 and 134 may be required for associating the core protein with the ER and the mitochondrial outer membrane. When amino acids 117 to 134 are portrayed as a helical wheel, we found an amphipathic structure with hydrophobic residues on one side and polar residues on the other side of the α-helix (Fig. 6C), which is often observed in membrane-associated proteins. This helical conformation might be important for directing the core protein to the ER and mitochondrial outer membranes.

**Nuclear localization of the HCV core protein is mediated by a bipartite NLS, possibly via an importin-dependent pathway.** Although HCV core protein is mainly localized within the cytoplasm, it is also found in the nucleus, as shown in Fig. 3.

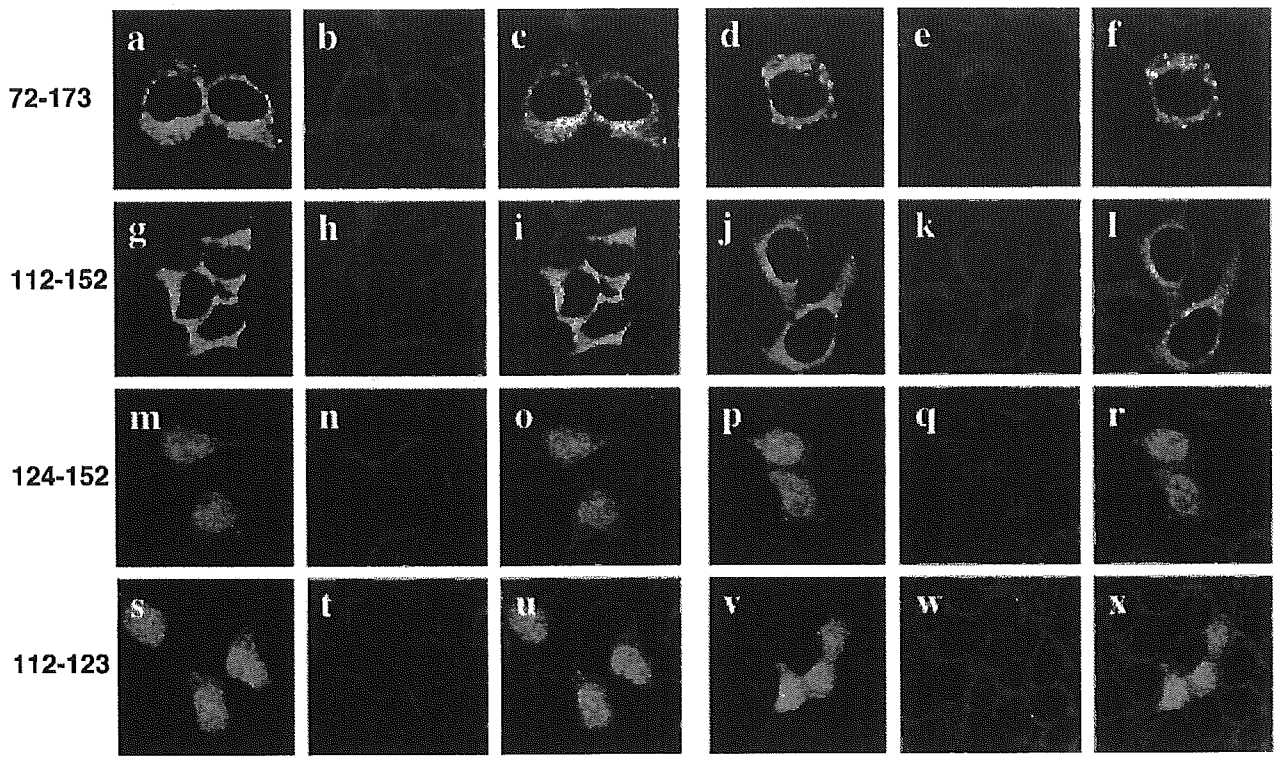


FIG. 5. Confocal analysis of double staining for core-GFP fusion protein and ER or mitochondria. 293T cells transfected with core-GFP expression plasmids (72–173, 112–152, 124–152, and 112–123) were allowed to express the plasmid for 2 days. Transfected cells were fixed directly (a to c, g to i, m to o, and s to u) or fixed after loading with Mitotracker (d to f, j to l, p to r, and v to x). After permeabilization with Triton X-100, a goat anticalregulin antibody was used for ER staining. The red signals corresponding to the ER were obtained with a rhodamine-conjugated rabbit anti-goat IgG secondary antibody (b, h, n, and t). Mitochondria were stained with the mitochondrion-selective dye Mitotracker (e, k, q, and w). Overlay resulted in yellow signals indicative of colocalization (c, f, i, l, o, r, u, and x).

The results of previous studies demonstrate that the N-terminal region of the core protein is responsible for nuclear targeting. It contains three clusters of basic amino acid residues that represent putative consensus motifs for NLS sequences PKPQRKTKR (amino acids 5 to 13), PRRGPR (amino acids 38 to 43), and PRGRRQPIPKARRP (amino acids 58 to 71) (6, 48). Nuclear targeting is generally governed by a family of transporters or cytosolic receptor proteins, known as importins or karyopherins, which function in concert with a guanine nucleotide-binding protein named Ran and other regulatory proteins such as NTF2/p10. Conventional NLS-dependent nuclear targeting occurs when importin-α recognizes the NLS sequence, mediating binding to importin-β1, after which the trimeric complex translocates to the nucleus (12).

In order to determine whether the putative NLS motifs identified within the core protein sequence are capable of binding to importin-α, we examined the in vitro interaction between bacterially expressed GST-fused core protein and $^{35}$S-labeled importin-α with a GST pulldown assay. We then substituted lysine and arginine residues of one or more of the putative NLS motifs of the core protein (all contained within the first 71 amino acids of the N terminus) with alanine and fused the resultant constructs with GST, as shown schematically in Fig. 7A. As shown in Fig. 7B (upper panel), importin-α was pulled down by a GST fusion protein containing wild-type core (amino acids 1 to 71) protein but not with GST alone, suggesting that direct binding occurs between the core protein and importin-α. Importin-α was also pulled down by GST-core fusion proteins containing substitutions in one or two NLS motifs (NLS/m1, NLS/m2, NLS/m3, NLS/m4, NLS/m5, and NLS/m6). However, importin-α was not pulled down by GST-core fusion proteins containing alanine substitutions in all three NLS motifs (NLS/m7). It should be noted that similar amounts of GST fusion proteins were used for each of the in vitro pulldown assays, followed by SDS-PAGE and Coomassie brilliant blue staining (Fig. 7B, lower panel). These results demonstrated that all three putative NLS motifs of the N-terminal region of the core protein can mediate binding to importin-α, which suggests that nuclear translocation of the core protein occurs via an importin-dependent pathway (12).

The interaction between the core and importin-α was further analyzed by a colocalization assay (Fig. 7C). The GFP fusion containing the wild-type core (amino acids 1 to 71) was well colocalized with HA-importin-α; distribution of the two proteins showed similar nuclear staining patterns, confirming the presence of a functional NLS sequence(s) within the core protein. In contrast, NLS/m4, with substitutions in two NLS motifs, was partly colocalized with HA-importin-α near or around the nuclear membrane, suggesting that NLS motif double mutants bind to importin-α but their binding efficiency is lower than that of wild-type core protein.

Finally, we examined the subcellular localization of core

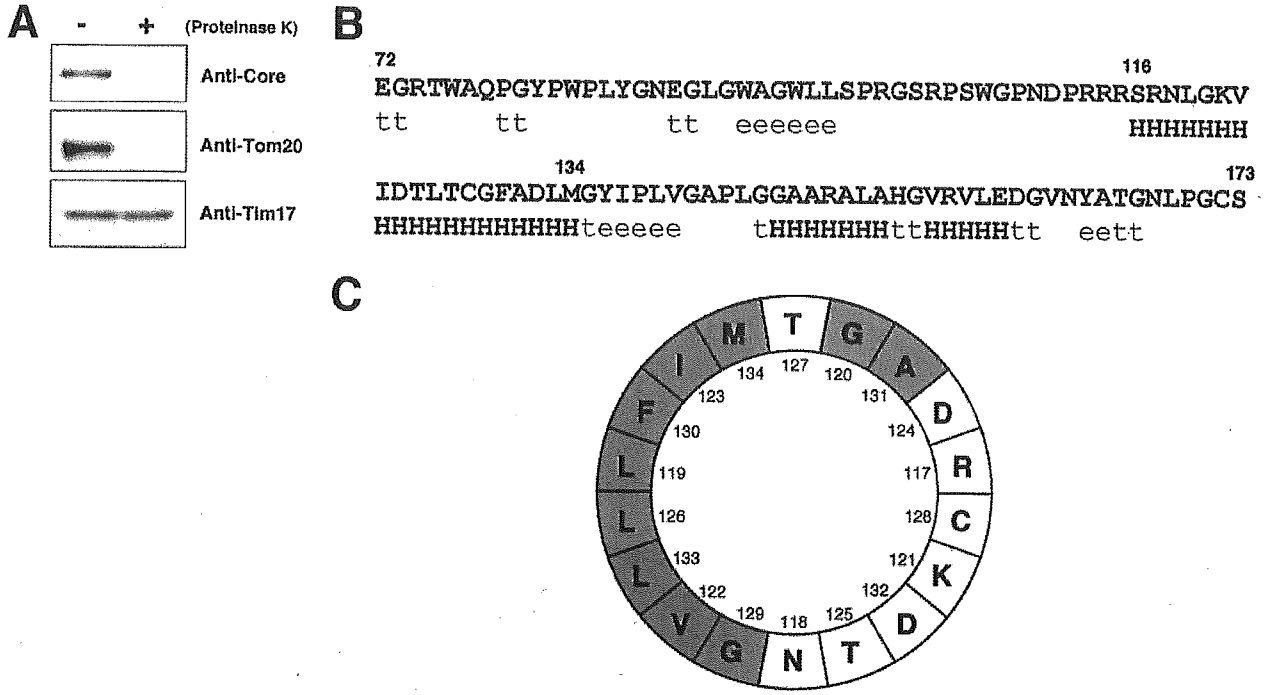


FIG. 6. (A) Protease protection assay. A mitochondrial fraction isolated from cells expressing the core protein was treated with proteinase K (+) as described in Materials and methods. The sample as well as the nontreated fraction (−) were subjected to immunoblotting with a monoclonal antibody against either HCV core, Tom20, or Tim17. (B) Protein sequence and predicted secondary structure of HCV core, amino acids 72 to 173. The secondary structure prediction was obtained with the self-optimized prediction method, a computer program on the internet (http://npsa-pbil.ibcp.fr/cgi-bin/npsa_automat.pl?page = /NPSA/npsa_sopm.html). H, α-helix; t, turn; e, extension. (C) α-Helical plot of amino acids 117 to 134 of the core protein. In the helical wheel plots, the gray shading represents apolar and hydrophobic residues; and the white represents polar residues.

protein expressed by the wild-type and NLS mutants (Fig. 7D). As expected, a fusion protein containing wild-type core protein (amino acids 1 to 71) and GFP was localized exclusively to the nucleus. Core proteins from three fusion proteins containing substitutions in each NLS motif (NLS/m1, NLS/m2, and NLS/m3) were detected primarily in the nucleus. Weak fluorescence was also observed in the cytoplasm, suggesting that these mutations caused a slight reduction in the efficiency of nuclear translocation. On the other hand, two or three NLS motif substitution mutations (NLS/m4, NLS/m5, NLS/m6, and NLS/m7) completely abolished nuclear translocation, resulting in a diffuse distribution of core protein, similar to that of GFP alone. Although it is likely that all three putative NLS motifs play a role, the above results suggest that at least two of the three putative NLS motifs are prerequisite for efficient nuclear translocation of the core protein.

## DISCUSSION

HCV core protein is released from the viral polyprotein by a host protease(s) within the ER membrane at a signal peptide sequence lying between the core and envelope (E1) proteins (16, 41). Subsequently, the signal peptide is further processed by an intramembranous protease called signal peptide peptidase (38, 53). This mature form of the core protein is then released and undergoes subcellular trafficking (30, 53). The core protein localizes mainly to the ER, mitochondria, and lipid droplets. Some reports also describe localization of the core protein to the nuclei of hepatocytes in HCV-infected patients (10), transgenic mice (34), and cultured cells expressing viral polyproteins (56). Although it has been reported which sequence motifs are responsible for localization of the HCV core protein to lipid droplets and nuclei, it is uncertain which sequences target the core protein to the ER and to mitochondria. In this study, we identified sequences related to localization of the mature core protein to the ER and to mitochondria.

Through heterologous expression of core-GFP fusion proteins containing a series of deletions, we determined that a sequence extending from amino acids 112 to 152 of the core protein is required for its localization at the mitochondrial outer membrane. Translocation of nucleus-encoded mitochondrial proteins is usually dependent on N-terminal sequences, referred to as mitochondrial targeting sequences (37). However, it is also true that a significant proportion of mitochondrial proteins lack these N-terminal mitochondrial targeting sequences. Specifically, a number of outer membrane proteins do not have cleavable sequences at their N termini; rather, they are targeted to mitochondria by means of internal or C-terminal signals (31).

Since it has been reported that amino acid sequences required for targeting to the outer mitochondrial membrane form a highly hydrophobic α-helical wheel, as seen in A-kinase associated protein 84/12 (4) and NADH-cytochrome *b* reduc-

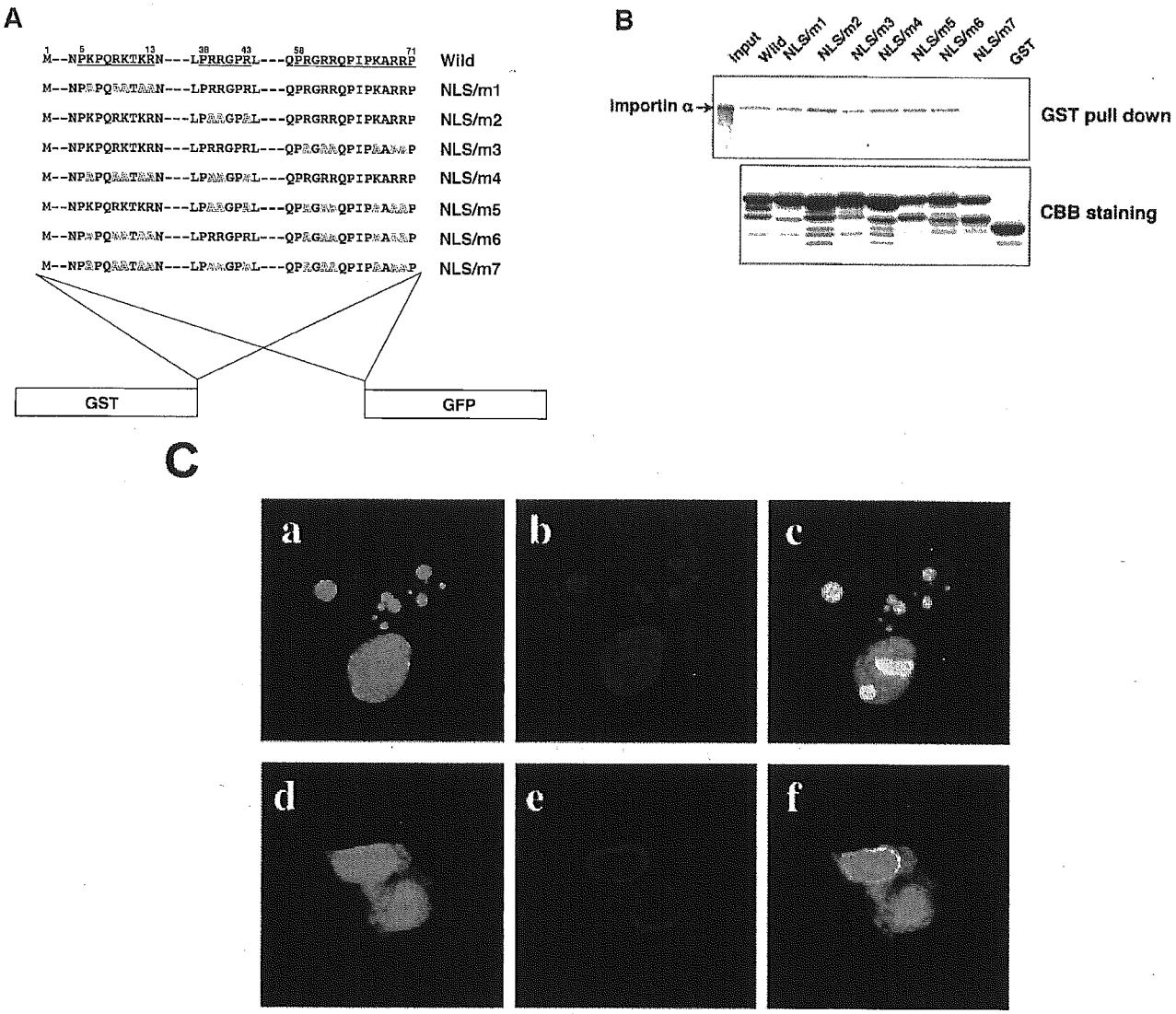


FIG. 7. Mutational analyses of NLS motifs in HCV core protein. (A) Schematic structures of fusion proteins and amino acid sequences corresponding to putative NLS motifs, three basic clusters (underlined) in the core protein. Two series of constructs fused with either GFP or GST were created. The mutated basic residues are indicated with outline letters. (B) GST pulldown assay. Equal amounts of GST fusions as described in A or GST alone was immobilized on glutathione-Sepharose 4B beads and incubated with in vitro-translated, [$^{35}$S]methionine-labeled importin-α. Bound material was separated by SDS-PAGE, and the amount of importin-α bound was detected by autoradiography. Direct electrophoretic separation of in vitro translation products served as a control (input). Coomassie brilliant blue staining of GST fusions and GST alone are shown in the bottom panel. (C) Confocal analysis of double staining for core-GFP fusion protein and HA-importin-α. 293T cells transfected with the wild-type core (1–71)-GFP (a to c) or NLS/m4 (d to f) expression plasmid and pCAG-HA-imp were allowed to express for 2 days. After the cells were fixed and permeabilized, they were incubated with a mouse anti-HA antibody. The red signals corresponding to HA-importin-α were obtained with a rhodamine-conjugated goat anti-mouse IgG secondary antibody (b and e). Overlay resulted in yellow signals indicative of colocalization (c and f). (D) Subcellular localization of GFP fusion proteins. GFP fusions with and without substitution mutations in the NLS motifs of the core protein as described in A were expressed in 293T cells. GFP images of the fixed cells were recorded.

tase (14), a predicted structure of an amphipathic α-helix present between amino acids 116 and 134 (Fig. 6B and C) possibly plays a role in directing the core protein to the mitochondrial outer membrane. Sequence comparisons demonstrate conservation of the amino acid sequence and secondary structure of the region, amino acids 112 to 152, among a variety of HCV isolates, including the infectious H77c clone (55), as well as a full-length adaptive replicon (3). To gain insight into the significance of the secondary structure of the region in targeting to the mitochondria, further structural and biochemical analyses are needed.

The association of HCV core protein with the mitochondrial membrane suggests that the core protein has the ability to modulate mitochondrial function, possibly by altering the permeability of the mitochondrial membrane. The core protein induces the production of cellular reactive oxygen species in

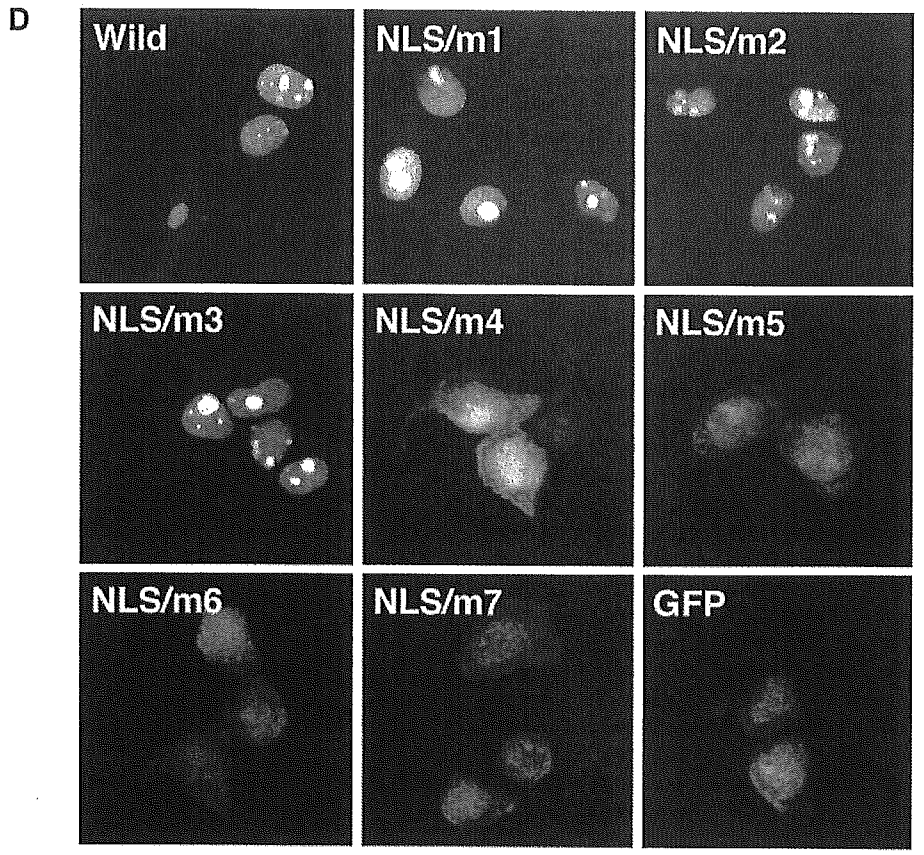


FIG. 7—*Continued.*

the livers of core-transgenic mice and in core-expressing cell lines (35). Reactive oxygen species, predominantly generated in mitochondria, induce genetic mutations and act as secondary messengers to regulate a variety of cellular functions, including gene expression and proliferation (1). Although the molecular mechanism by which core protein induces reactive oxygen species production is still unclear, HCV core protein is known to impair the mitochondrial electron transfer system (35). The core protein may also modulate apoptosis, since mitochondria play a major role in regulating programmed cell death. Expression of HCV proteins, including the core protein, suppresses the release of cytochrome *c* from mitochondria to the cytoplasm in HCV-transgenic mice, thus inhibiting Fas-mediated apoptosis (27).

Okamoto et al. recently reported that not only the C-terminal signal sequence but also amino acids 128 to 151 are required for ER retention of the core protein by using a series of N-terminally truncated core protein constructs (38). Here, in this study, we further showed that amino acids 112 to 152 mediate association of the core protein with the ER in the absence of the C-terminal signal sequence. Hope and McLauchlan demonstrated that the central domain of the core protein, amino acids 119 to 174, is important for association with lipid droplets (17). They also showed that this corresponding domain is shared with GB virus B, which is most closely related to HCV, but not with either pestiviruses or flaviviruses (18). It appears that the 41 residues identified as the sequence mediating association with the ER membrane in the present study are crucial for directing the core protein to lipid droplets, since the surface of lipid droplets must derive from the cytoplasmic side of the ER membrane.

The HCV core protein contains NLS sequences which are composed of three stretches of sequences rich in basic residues. These sequences were originally identified by experiments with fused forms of wild-type and mutated core proteins with β-galactosidase (6, 48). C-terminally truncated versions of the core protein localize exclusively to the nucleus (48). A fraction of the core protein is detected in the nucleus even when full-length HCV core gene is expressed (Fig. 2) and as described (34, 56). However, it is difficult to demonstrate clearly the nuclear localization of the core protein by immunofluorescence, presumably because of the instability of nuclearly localized core protein (49, 33). We only observed a nuclear staining pattern of the matured core protein after adding proteasome inhibitors to the culture (33).

Generally, NLS sequences fall into two categories; (i) monopartite NLSs, which contain a single cluster of basic residues, and (ii) bipartite NLSs, which contain two clusters of basic residues separated by an unconserved linker sequence of variable length (reviewed in reference 12). Nuclear translocation of an NLS-containing cargo protein is initiated when the soluble import receptor (importin) recognizes the NLS-contain-

ing protein within the cytoplasm. Importin-α contains an NLS-binding site(s), and importin-β docks importin-cargo complexes to the cytoplasmic filaments of a nuclear pore complex, after which translocation occurs through the nuclear pore. Thus, importin-α functions as an adaptor between the bona fide import receptor and the NLS-containing protein.

We further characterized the NLS of the core protein and found that each of the NLS motifs of the core protein is able to bind to importin-α and that at least two NLS motifs are required for efficient nuclear distribution of the core protein in cells. It appears that double mutations among three NLS motifs decrease the ability of the core protein to bind importin-α. These observations suggest that the binding of the double mutants with importin-α leads to no or little active translocation of the core protein into the nucleus. The double mutations may also block subsequent interactions with importin-β1, GTPase Ran, and/or NTF2/p10, which are required for translocation through the nuclear pore complexes.

The findings obtained in this study suggest that HCV core protein NLS motifs have a bipartite function. Crystallographic studies of monopartite (e.g., simian virus 40 large T antigen) and bipartite (e.g., nucleoplasmin) NLSs show that the basic residue clusters of bipartite NLSs occupy separate binding sites on importin-α. In contrast, while monopartite NLSs can bind to the same sites as bipartate NLSs on importin-α, they mainly bind to the N-terminal binding site, which is referred to as the major binding site on importin-α (9, 11). A recent report describes an importin-α variant with a mutation in the major site which results in decreased ability to bind both monopartite and bipartite NLSs. Another variant with a mutation in the minor site exhibits decreased binding only to bipartite NLS-containing proteins, making importin-α nonfunctional in vivo (22). Thus, we favor a model in which the core protein bipartite NLS, composed of any two of the three basic clusters, occupies both major and minor binding sites on importin-α, resulting in efficient nuclear translocation. Importin-α may be equally accessible to all clusters, given their close proximity to one another, as well as the distinct conformational flexibility of the ≈70-residue N-terminal region of the core protein.

With regard to the molecular mechanisms participating in nuclear localization of the core protein, Moriishi et al. found that PA28γ is involved in nuclear localization of the core protein. Interaction of the core protein with PA28γ plays an important role in retention of the core protein in the nucleus (33). Furthermore, in yeast cells, nuclear transport of the core protein requires the activity of the small GTPase Ran/Gsp1p and is mediated by Kap123p, but neither importin-α nor importin-β is involved (20). Differences in nucleocytoplasmic transport between yeast and mammalian cells might explain the inconsistencies observed in the present study. Further experiments are required to characterize the exact nature of the interaction between the core protein and components of the nuclear import machinery, particularly in cells where HCV is replicating.

In conclusion, the mature HCV core protein has an internal 41-amino-acid sequence mediating association of the viral protein with the ER and mitochondria. We also provide evidence for a novel class of bipartite NLS contained within the core protein, which comprises two of three basic motifs, thus enabling efficient nuclear targeting. Multiple functional domains influence the subcellular localization of the core protein, which ultimately depends on the balance of the respective signals.

## ACKNOWLEDGMENTS

We thank colleagues in the laboratories of the Department of Virology II at the National Institute of Infectious Diseases of Japan for providing advice and help. We especially thank Mami Matsuda and Makiko Yahata for assistance in sequencing and the preparation of experimental reagents and Tomoko Mizoguchi for secretarial work. We are grateful to Karsten Weis for providing us with the plasmid containing importin-α cDNA.

This work was supported in part by Second Term Comprehensive 10-Year Strategy for Cancer Control and Research on Emerging and Reemerging Infectious Diseases, Health Sciences Research Grants of the Ministry of Health, Labor and Welfare, and by the Program for Promotion of Fundamental Studies in Health Sciences of the Organization for Drug ADR Relief, R&D Promotion and Product Review of Japan (ID:01–3). This work was also supported in part by a Grant-in-Aid for Young Scientists from the Ministry of Education, Culture, Sports, Science and Technology to R.S. (15790244).

## REFERENCES

1. **Adler, V., Z. Yin, K. D. Tew, and Z. Ronai.** 1999. Role of redox potential and reactive oxygen species in stress signaling. Oncogene **18**:6104–6111.
2. **Barba, G., F. Harper, T. Harada, M. Kohara, S. Goulinet, Y. Matsuura, G. Eder, Z. Schaff, M. J. Chapman, T. Miyamura, and C. Bréchot.** 1997. Hepatitis C virus core protein shows a cytoplasmic localization and associates to cellular lipid storage droplets. Proc. Natl. Acad. Sci. USA **94**:1200–1205.
3. **Bukh, J., T. Pietschmann, V. Lohmann, N. Krieger, K. Faulk, R. E. Engle, S. Govindarajan, M. Shapiro, M. St Claire, and R. Bartenschlager.** 2002. Mutations that permit efficient replication of hepatitis C virus RNA in Huh-7 cells prevent productive replication in chimpanzees. Proc. Natl. Acad. Sci. USA **99**:14416–14421.
4. **Cardone, L., T. de Cristofaro, A. Affaitati, C. Garbi, M. D. Ginsberg, M. Saviano, S. Varrone, C. S. Rubin, M. E. Gottesman, E. V. Avvedimento, and A. Feliciello.** 2002. A-kinase anchor protein 84/121 are targeted to mitochondria and mitotic spindles by overlapping amino-terminal motifs. J. Mol. Biol. **320**:663–675.
5. **Chang, J., S. H. Yang, Y. G. Cho, S. B. Hwang, Y. S. Hahn, and Y. C. Sung.** 1998. Hepatitis C virus core from two different genotypes has an oncogenic potential but is not sufficient for transforming primary rat embryo fibroblasts in cooperation with the H-ras oncogene. J. Virol. **72**:3060–3065.
6. **Chang, S. C., J. H. Yen, H. Y. Kang, M. H. Jang, and M. F. Chang.** 1994. Nuclear localization signals in the core protein of hepatitis C virus. Biochem. Biophys. Res. Commun. **205**:1284–1290.
7. **Choo, Q. L., G. Kuo, A. J. Weiner, L. R. Overby, D. W. Bradley, and M. Houghton.** 1989. Isolation of a cDNA clone derived from a blood-borne non-A, non-B viral hepatitis genome. Science **244**:359–362.
8. **Choo, Q. L., K. H. Richman, J. H. Han, K. Berger, C. Lee, C. Dong, C. Gallegos, D. Coit, R. Medina-Selby, P. J. Barr, et al.** 1991. Genetic organization and diversity of the hepatitis C virus. Proc. Natl. Acad. Sci. USA **88**:2451–2455.
9. **Conti, E., M. Uy, L. Leighton, G. Blobel, and J. Kuriyan.** 1998. Crystallographic analysis of the recognition of a nuclear localization signal by the nuclear import factor karyopherin alpha. Cell **94**:193–204.
10. **Falcon, V., N. Acosta-Rivero, G. Chinea, M. C. de la Rosa, I. Menendez, S. Duenas-Carrera, B. Gra, A. Rodriguez, V. Tsutsumi, M. Shibayama, J. Luna-Munoz, M. M. Miranda-Sanchez, J. Morales-Grillo, and J. Kouri.** 2003. Nuclear localization of nucleocapsid-like particles and HCV core protein in hepatocytes of a chronically HCV-infected patient. Biochem. Biophys. Res. Commun. **310**:54–58.
11. **Fontes, M. R., T. Teh, and B. Kobe.** 2000. Structural basis of recognition of monopartite and bipartite nuclear localization sequences by mammalian importin-alpha. J. Mol. Biol. **297**:1183–1194.
12. **Görlich, D., and U. Kutay.** 1999. Transport between the cell nucleus and the cytoplasm. Annu. Rev. Cell. Dev. Biol. **15**:607–660.
13. **Grakoui, A., D. W. McCourt, C. Wychowski, S. M. Feinstone, and C. M. Rice.** 1993. Characterization of the hepatitis C virus-encoded serine proteinase: determination of proteinase-dependent polyprotein cleavage sites. J. Virol. **67**:2832–2843.
14. **Hahne, K., V. Haucke, L. Ramage, and G. Schatz.** 1994. Incomplete arrest in the outer membrane sorts NADH-cytochrome b5 reductase to two different submitochondrial compartments. Cell **79**:829–839.
15. **Harada, S., Y. Watanabe, K. Takeuchi, T. Suzuki, T. Katayama, Y. Takebe, I. Saito, and T. Miyamura.** 1991. Expression of processed core protein of hepatitis C virus in mammalian cells. J. Virol. **65**:3015–3021.
16. **Hijikata, M., N. Kato, Y. Ootsuyama, M. Nakagawa, and K. Shimotohno.** 1991. Gene mapping of the putative structural region of the hepatitis C virus

genome by in vitro processing analysis. Proc. Natl. Acad. Sci. USA **88**:5547–5551.
17. **Hope, R. G., and J. McLauchlan.** 2000. Sequence motifs required for lipid droplet association and protein stability are unique to the hepatitis C virus core protein. J. Gen. Virol. **81**:1913–1925.
18. **Hope, R. G., D. J. Murphy, and J. McLauchlan.** 2002. The domains required to direct core proteins of hepatitis C virus and GB virus-B to lipid droplets share common features with plant oleosin proteins. J. Biol. Chem. **277**:4261–4270.
19. **Hüssy, P., H. Langen, J. Mous, and H. Jacobsen.** 1996. Hepatitis C virus core protein: carboxy-terminal boundaries of two processed species suggest cleavage by a signal peptide peptidase. Virology **224**:93–104.
20. **Isoyama, T., S. Kuge, and A. Nomoto.** 2002. The core protein of hepatitis C virus is imported into the nucleus by transport receptor Kap123p but inhibits Kap121p-dependent nuclear import of yeast AP1-like transcription factor in yeast cells. J. Biol. Chem. **277**:39634–39641.
21. **Lai, M. M., and C. F. Ware.** 2000. Hepatitis C virus core protein: possible roles in viral pathogenesis. Curr. Top. Microbiol. Immunol. **242**:117–134.
22. **Leung, S. W., M. T. Harreman, M. R. Hodel, A. E. Hodel, and A. H. Corbett.** 2003. Dissection of the karyopherin alpha nuclear localization signal (NLS)-binding groove: functional requirements for NLS binding. J. Biol. Chem. **278**:41947–41953.
23. **Liu, Q., C. Tackney, R. A. Bhat, A. M. Prince, and P. Zhang.** 1997. Regulated processing of hepatitis C virus core protein is linked to subcellular localization. J. Virol. **71**:657–662.
24. **Lo, S. Y., F. Masiarz, S. B. Hwang, M. M. Lai, and J. H. Ou.** 1995. Differential subcellular localization of hepatitis C virus core gene products. Virology **213**:455–461.
25. **Lo, S. Y., M. Selby, M. Tong, and J. H. Ou.** 1994. Comparative studies of the core gene products of two different hepatitis C virus isolates: two alternative forms determined by a single amino acid substitution. Virology **199**:124–131.
26. **Lu, W., A. Strohecker, and J. H. Ou.** 2001. Post-translational modification of the hepatitis C virus core protein by tissue transglutaminase. J. Biol. Chem. **276**:47993–47999.
27. **Machida, K., K. Tsukiyama-Kohara, E. Seike, S. Tone, F. Shibasaki, M. Shimizu, H. Takahashi, Y. Hayashi, N. Funata, C. Taya, H. Yonekawa, and M. Kohara.** 2001. Inhibition of cytochrome c release in Fas-mediated signaling pathway in transgenic mice induced to express hepatitis C viral proteins. J. Biol. Chem. **276**:12140–12146.
28. **Matsumoto, M., S. B. Hwang, K. S. Jeng, N. Zhu, and M. M. Lai.** 1996. Homotypic interaction and multimerization of hepatitis C virus core protein. Virology **218**:43–51.
29. **McLauchlan, J.** 2000. Properties of the hepatitis C virus core protein: a structural protein that modulates cellular processes. J. Viral Hepatitis **7**:2–14.
30. **McLauchlan, J., M. K. Lemberg, G. Hope, and B. Martoglio.** 2002. Intramembrane proteolysis promotes trafficking of hepatitis C virus core protein to lipid droplets. EMBO J. **21**:3980–3988.
31. **Mihara, K.** 2000. Targeting and insertion of nuclear-encoded preproteins into the mitochondrial outer membrane. Bioessays **22**:364–371.
32. **Moradpour, D., C. Englert, T. Wakita, and J. R. Wands.** 1996. Characterization of cell lines allowing tightly regulated expression of hepatitis C virus core protein. Virology **222**:51–63.
33. **Moriishi, K., T. Okabayashi, K. Nakai, K. Moriya, K. Koike, S. Murata, T. Chiba, K. Tanaka, R. Suzuki, T. Suzuki, T. Miyamura, and Y. Matsuura.** 2003. Proteasome activator PA28gamma-dependent nuclear retention and degradation of hepatitis C virus core protein. J. Virol. **77**:10237–10249.
34. **Moriya, K., H. Fujie, Y. Shintani, H. Yotsuyanagi, T. Tsutsumi, K. Ishibashi, Y. Matsuura, S. Kimura, T. Miyamura, and K. Koike.** 1998. The core protein of hepatitis C virus induces hepatocellular carcinoma in transgenic mice. Nat. Med. **4**:1065–1067.
35. **Moriya, K., K. Nakagawa, T. Santa, Y. Shintani, H. Fujie, H. Miyoshi, T. Tsutsumi, T. Miyazawa, K. Ishibashi, T. Horie, K. Imai, T. Todoroki, S. Kimura, and K. Koike.** 2001. Oxidative stress in the absence of inflammation in a mouse model for hepatitis C virus-associated hepatocarcinogenesis. Cancer Res. **61**:4365–4370.
36. **Moriya, K., H. Yotsuyanagi, Y. Shintani, H. Fujie, K. Ishibashi, Y. Matsuura, T. Miyamura, and K. Koike.** 1997. Hepatitis C virus core protein induces hepatic steatosis in transgenic mice. J. Gen. Virol. **78**:1527–1531.
37. **Neupert, W.** 1997. Protein import into mitochondria. Annu. Rev. Biochem. **66**:863–917.
38. **Okamoto, K., K. Moriishi, T. Miyamura, and Y. Matsuura.** 2004. Intramembrane proteolysis and endoplasmic reticulum retention of hepatitis C virus core protein. J. Virol. **78**:6370–6380.
39. **Okuda, M., K. Li, M. R. Beard, L. A. Showalter, F. Scholle, S. M. Lemon, and S. A. Weinman.** 2002. Mitochondrial injury, oxidative stress, and antioxidant gene expression are induced by hepatitis C virus core protein. Gastroenterology **122**:366–375.
40. **Perlemuter, G., A. Sabile, P. Letteron, G. Vona, A. Topilco, Y. Chretien, K. Koike, D. Pessayre, J. Chapman, G. Barba, and C. Bréchot.** 2002. Hepatitis C virus core protein inhibits microsomal triglyceride transfer protein activity and very low density lipoprotein secretion: a model of viral-related steatosis. FASEB J. **16**:185–194.
41. **Ralston, R., K. Thudium, K. Berger, C. Kuo, B. Gervase, J. Hall, M. Selby, G. Kuo, M. Houghton, and Q. L. Choo.** 1993. Characterization of hepatitis C virus envelope glycoprotein complexes expressed by recombinant vaccinia viruses. J. Virol. **67**:6753–6761.
42. **Ray, R. B., L. M. Lagging, K. Meyer, and R. Ray.** 1996. Hepatitis C virus core protein cooperates with ras and transforms primary rat embryo fibroblasts to tumorigenic phenotype. J. Virol. **70**:4438–4443.
43. **Roth, J., D. J. Taatjes, and M. J. Warhol.** 1989. Prevention of non-specific interactions of gold-labeled reagents on tissue sections. Histochemistry **92**: 47–56.
44. **Sabile, A., G. Perlemuter, F. Bono, K. Kohara, F. Demaugre, M. Kohara, Y. Matsuura, T. Miyamura, C. Brechot, and G. Barba.** 1999. Hepatitis C virus core protein binds to apolipoprotein AII and its secretion is modulated by fibrates. Hepatology **30**:1064–1076.
45. **Santolini, E., G. Migliaccio, and N. La Monica.** 1994. Biosynthesis and biochemical properties of the hepatitis C virus core protein. J. Virol. **68**: 3631–3641.
46. **Selby, M. J., Q. L. Choo, K. Berger, G. Kuo, E. Glazer, M. Eckart, C. Lee, D. Chien, C. Kuo, and M. Houghton.** 1993. Expression, identification and subcellular localization of the proteins encoded by the hepatitis C viral genome. J. Gen. Virol. **74**:1103–1113.
47. **Shimoike, T., S. Mimori, H. Tani, Y. Matsuura, and T. Miyamura.** 1999. Interaction of hepatitis C virus core protein with viral sense RNA and suppression of its translation. J. Virol. **73**:9718–9725.
48. **Suzuki, R., Y. Matsuura, T. Suzuki, A. Ando, J. Chiba, S. Harada, I. Saito, and T. Miyamura.** 1995. Nuclear localization of the truncated hepatitis C virus core protein with its hydrophobic C terminus deleted. J. Gen. Virol. **76**:53–61.
49. **Suzuki, R., K. Tamura, J. Li, K. Ishii, Y. Matsuura, T. Miyamura, and T. Suzuki.** 2001. Ubiquitin-mediated degradation of hepatitis C virus core protein is regulated by processing at its carboxyl terminus. Virology **280**:301–309.
50. **Tanaka, Y., T. Shimoike, K. Ishii, R. Suzuki, T. Suzuki, H. Ushijima, Y. Matsuura, and T. Miyamura.** 2000. Selective binding of hepatitis C virus core protein to synthetic oligonucleotides corresponding to the 5′ untranslated region of the viral genome. Virology **270**:229–236.
51. **Tellinghuisen, T. L., and C. M. Rice.** 2002. Interaction between hepatitis C virus proteins and host cell factors. Curr. Opin. Microbiol. **5**:419–427.
52. **Thomson, M., and T. J. Liang.** 2000. Molecular biology of hepatitis C virus, p. 1–23. *In* T. J. Liang and J. H. Hoofnagle (ed.), Hepatitis C. Academic Press, San Diego, Calif.
53. **Weihofen, A., K. Binns, M. K. Lemberg, K. Ashman, and B. Martoglio.** 2002. Identification of signal peptide peptidase, a presenilin-type aspartic protease. Science **296**:2215–2218.
54. **Weis, K., I. W. Mattaj, and A. I. Lamond.** 1995. Identification of hSRP1 alpha as a functional receptor for nuclear localization sequences. Science **268**:1049–1053.
55. **Yanagi, M., R. H. Purcell, S. U. Emerson, and J. Bukh.** 1997. Transcripts from a single full-length cDNA clone of hepatitis C virus are infectious when directly transfected into the liver of a chimpanzee. Proc. Natl. Acad. Sci. USA **94**:8738–8743.
56. **Yasui, K., T. Wakita, K. Tsukiyama-Kohara, S. I. Funahashi, M. Ichikawa, T. Kajita, D. Moradpour, J. R. Wands, and M. Kohara.** 1998. The native form and maturation process of hepatitis C virus core protein. J. Virol. **72**:6048–6055.

JOURNAL OF VIROLOGY, Mar. 2005, p. 3639–3652
0022-538X/05/$08.00+0 doi:10.1128/JVI.79.6.3639–3652.2005

Vol. 79, No. 6

# Ligand-Directed Gene Targeting to Mammalian Cells by Pseudotype Baculoviruses†

Yoshinori Kitagawa, Hideki Tani, Chang Kwang Limn, Tomoko M. Matsunaga, Kohji Moriishi, and Yoshiharu Matsuura*

*Research Center for Emerging Infectious Diseases, Research Institute for Microbial Diseases, Osaka University, Osaka, Japan*

Received 27 August 2004/Accepted 25 October 2004

**The baculovirus *Autographa californica* multiple nucleopolyhedrovirus (AcMNPV) can infect a variety of mammalian cells, as well as insect cells, facilitating its use as a viral vector for gene delivery into mammalian cells. Glycoprotein gp64, a major component of the budded AcMNPV envelope, is involved in viral entry into cells by receptor-mediated endocytosis and subsequent membrane fusion. We examined the potential production of pseudotype baculovirus particles transiently carrying ligands of interest in place of gp64 as a method of ligand-directed gene delivery into target cells. During amplification of a gp64-null pseudotype baculovirus carrying a green fluorescent protein gene in gp64-expressing insect cells, however, we observed the high-frequency appearance of a replication-competent virus incorporating the gp64 gene into the viral genome. To avoid generation of replication-competent revertants, we prepared pseudotype baculoviruses by transfection with recombinant bacmids without further amplification in the gp64-expressing cells. We constructed gp64-null recombinant bacmids carrying cDNAs encoding either vesicular stomatitis virus G protein (VSVG) or measles virus receptors (CD46 or SLAM). The VSVG pseudotype baculovirus efficiently transduced a reporter gene into a variety of mammalian cell lines, while CD46 and SLAM pseudotype baculoviruses allowed ligand-receptor-directed reporter gene transduction into target cells expressing measles virus envelope glycoproteins. Gene transduction mediated by the pseudotype baculoviruses could be inhibited by pretreatment with specific antibodies. These results indicate the possible application of pseudotype baculoviruses in ligand-directed gene delivery into target cells.**

The baculovirus *Autographa californica* multiple nucleopolyhedrovirus (AcMNPV) is an insect virus possessing a 134-kb double-stranded circular DNA genome (3). Due to the strong polyhedrin and p10 promoters, baculovirus is commonly used as a tool for the large-scale production of recombinant protein in insect cells (32, 38). Baculovirus is also capable of entering into a variety of mammalian cells to facilitate the expression of foreign genes under the control of the mammalian promoters without replication of the viral genome (8, 21, 61). Therefore, baculovirus is a useful viral vector, not only for the abundant expression of foreign genes in insect cells, but also for efficient gene delivery to mammalian cells (29). AcMNPV has a number of unique beneficial properties as a viral vector, including a large capacity for foreign gene incorporation, easy manipulation, and replication competence in insect cells combined with incompetence in mammalian cells. Therefore, the possibility of generating replication-competent revertants expressing baculoviral gene products, which can often lead to harmful immune responses against mammalian cells, is significantly lower than for other viral vectors presently in use. Furthermore, studies of host responses to baculovirus infection in vivo revealed that AcMNPV can stimulate interferon production in mammalian cell lines, conferring protection from lethal encephalomyocarditis virus infections in mice (18). Intranasal inoculation with AcMNPV also induces a strong innate immune response, protecting mice from lethal challenges of influenza A or B virus (1). The precise mechanism of protective immune response induction by AcMNPV, however, remains unclear.

Recently, several groups have reported enhanced gene transfer in a variety of cell lines infected with recombinant baculoviruses expressing either foreign viral envelope proteins, such as vesicular stomatitis virus envelope G protein (VSVG), or excess amounts of the endogenous envelope glycoprotein, gp64, on the virion surface (4, 65, 66). Although modification of the virion surface enhances the efficiency of gene transduction into a variety of cell lines, the utility of recombinant baculoviruses in cell-type-specific gene transduction is still unsatisfactory. Ojala et al. demonstrated that, while baculoviruses bearing either a single chain antibody fragment specific for carcinoembryonic antigen or a synthetic immunoglobulin G (IgG) binding domain derived from protein A could specifically bind target cells, cell type-specific gene transduction was unsuccessful (44, 45). Although gp64-null pseudotype baculoviruses expressing a foreign viral envelope protein, such as VSVG or fusion envelope glycoproteins from other baculoviruses, exhibited high infectivity to insect cells, their capacity for gene transduction into mammalian cells has yet to be explored (33, 34). The inefficiency of present gene transfer vectors in gaining entry into cells needing treatment can be problematic, as many therapeutic genes may be deleterious if delivered to bystander cells. Therefore, the development of a ligand-directed gene delivery vector capable of distinguishing between

* Corresponding author. Mailing address: Research Center for Emerging Infectious Diseases, Research Institute for Microbial Diseases, Osaka University, Osaka 565-0871, Japan. Phone: 81-6-6879-8340. Fax: 81-6-6879-8269. E-mail: matsuura@biken.osaka-u.ac.jp.

† This study is dedicated to the memory of Ikuko Yanase

target and nontarget tissue is essential for both the safety and efficacy of gene therapy.

In this study, we examined the stability of a generated gp64-null pseudotype baculovirus possessing the green fluorescent protein (GFP) gene during passages in insect cells stably expressing the gp64 protein. Replication-competent revertant viruses emerged with high frequency during passage in the cell line, incorporating the gp64 gene into the revertants' viral genomes. To overcome the emergence of revertant viruses during passage, we generated recombinant bacmids lacking the gp64 gene and carrying a ligand of interest and a reporter gene under the control of the polyhedrin and the CAG promoters, respectively. Pseudotype baculoviruses generated from these bacmids exhibited specific ligand-directed gene delivery into target cells. These pseudotype baculovirus vectors may be useful in future clinical gene targeting.

## MATERIALS AND METHODS

**Cells.** *Spodoptera frugiperda* (Sf9) cells were grown in TC-100 medium (Sigma, St. Louis, Mo.) supplemented with 0.26% tryptose phosphate broth (Difco, Detroit, Mich.) and 10% (vol/vol) fetal bovine serum (FBS) (Sigma) (66). To establish a cell line constitutively expressing gp64, Sf9 cells were transfected with pAFgp64 (see below) and pIB/V5-His (Invitrogen, Carlsbad, Calif.) using UniFector reagent (B-Bridge, Sunnyvale, Calif.). Thirty-six hours after transfection, Sf9 cells were selected in TC-100 medium containing blasticidin (50 μg/ml; Invitrogen). Resistant cells were stained with anti-gp64 antibodies (AcV1) (kindly provided by P. Faulkner) (22); positive cells were sorted using a FACSCalibur (Becton Dickinson, Franklin Lakes, N.J.) to establish a cell line, Sfgp64, stably expressing gp64 at the cell surface. The human embryonic kidney cell line 293T and the hamster kidney cell line BHK, purchased from the American Type Culture Collection, were maintained in Dulbecco's modified Eagle's medium (Sigma) containing 2 mM L-glutamine, penicillin (50 IU/ml), streptomycin (50 μg/ml), and 10% FBS (66).

**Construction of plasmids.** We constructed two expression plasmids, pAF-MCS1 and pAF-MCS2, harboring the A3 actin promoter, a multiple cloning site, and the polyadenylation signal derived from the *Bombyx mori* fibroin H-chain gene, for the subcloning of ligand molecules. First, the promoter and polyadenylation signal were excised from pA3Fb-Luc, kindly provided by H. Bando (Hokkaido University, Sapporo, Japan), and inserted into pUC18. To generate pAFgp64, the gp64 gene was excised from pFBgp64 (see below) by digestion with SalI and HindIII. This fragment was then inserted into the SalI-HindIII site of pAF-MCS1. Recombinant baculoviruses were constructed using the transfer vector pFASTBAC1 (Invitrogen). To measure the expression of foreign genes in mammalian cells, the firefly luciferase gene under the control of the CAG promoter (43) was subcloned into pFASTBAC1. To construct the transfer vector pFBCAluc, the CAG-luciferase cassette was excised from pCAGluc (61) by digestion with SalI, extension with Klenow enzyme, and redigestion with BamHI and inserted into the SnaBI-BamHI site of pFASTBAC1.

pUCgp64locus was generated by cloning the EcoRI-SmaI fragment from AcMNPV genomic DNA (corresponding to 107,325 to 112,041 nt) (3) into the EcoRI-SmaI site of pUC18. To generate pUCgp64, a fragment encoding the gp64 gene was excised from pUCgp64locus by digestion with SpeI and BglII and then cloned into the XbaI-BamHI site of pUC18. The gp64 gene was excised from pUCgp64 by digestion with SalI and KpnI and inserted into the SalI-KpnI site of pFASTBAC1. The resulting plasmid was designated pFBgp64. To generate pFBgp64CAluc, the cassette including the polyhedrin promoter and the gp64 gene was excised from pFBgp64 by digestion with SnaBI and KpnI and cloned into pFBCAluc, which was digested with SalI, extended with Klenow enzyme, and redigested with KpnI. The VSVG gene fragment was excised from pCAG-VSVG (64) by digestion with EcoRI and cloned into the EcoRI site of pFASTBAC1 to create pFBVSVG. pFBGFP was constructed by excision of the GFP gene from pAcVSVG-CAGFP (65) by digestion with EcoRI and subsequent insertion into the EcoRI site of pFASTBAC1. To generate pFBVSVGCAluc and pFBGFPCAluc, the DNA fragment encoding the polyhedrin promoter and either the VSVG or GFP gene was excised from pFBVSVG or pFBGFP, respectively, by digestion with SnaBI and XhoI and cloned into pFBCAluc, which was digested with SalI, extended with Klenow enzyme, and redigested with XhoI.

cDNAs encoding human CD46 and signaling lymphocyte activation molecule (SLAM; also known as CDw150) were amplified from the genomic DNAs of CHO/CD46 (kindly provided by T. Seya) (25) and CHO.SLAM (kindly provided by Y. Yanagi) (67) cells, respectively, by PCR. The CD46-Fw (1st) (5′-TTT CCTCCGGAGAAATAACAGC-3′) and CD46-Rv (1st) (5′-CTAAGCCAC AGTTGCACTCATG-3′) primers were used to amplify CD46 cDNA, and the SLAM-Fw (1st) (5′-TGACACGAAGCTTGCTTCTG-3′) and SLAM-Rv (1st) (5′-GTCGACCTTTGTTGGTCTCTGGTG-3′) primers were used to amplify SLAM cDNA. These PCR products were used as templates for a second PCR with the primers CD46-Fw-*Hind*III (5′-CCCCAAGCTTCCGCGCCGCG CATGGG-3′) and CD46-Rv-*Sal*I (5′-TTTTGTCGACTCAGCCTCTCTGCTC TGCTG-3′) to amplify CD46 cDNA and SLAM-Fw-*Hind*III (5′-CCCCAAGC TTCCTCATTGGCTGATGGATC-3′) and SLAM-Rv-*Sal*I (5′-AAAAGTCGA CTCAGCTCTCTGGAAGTGTCA-3′) to amplify SLAM cDNA. The amplified CD46 and SLAM cDNAs were digested with HindIII and SalI and then cloned into the HindIII-SalI sites of pAF-MCS2 to create pAFCD46 and pAFSLAM, respectively. The CD46 and SLAM cDNAs were excised from pAFCD46 and pAFSLAM, respectively, by digestion with HindIII, extension with Klenow enzyme, and redigestion with XbaI and cloned into pFASTBAC1. To generate pFBCD46CAluc and pFBSLAMCAluc, the DNA fragments encoding the polyhedrin promoter and either the CD46 gene or the SLAM gene were excised from pFBCD46 or pFBSLAM, respectively, by digestion with SnaBI and PvuI and cloned into pFBCAluc. A mutant SLAM gene, SLAMcyto7, possessing a truncated cytoplasmic domain of 7 amino acids, was generated by PCR with the primers SLAM-Fw-SmaI (5′-CCCCCCGGGCCTCATTGGCTGATGGATC-3′) and SLAM-7aa-stop-Rv-*Sal*I (5′-GGGGGGTCGACTCAGTTCGTTTT ACCTCTTCTTCTCAAC-3′). This PCR product was digested with SmaI and SalI and then cloned into the SmaI-SalI sites of pAF-MCS1 to create pAFSLAMcyto7. To construct pFBSLAMcyto7CAluc, the SLAMcyto7 gene was excised from pAFSLAMcyto7 and substituted for the full-length SLAM gene of pFBSLAMCAluc. All plasmids containing PCR-derived sequences were confirmed by sequence analyses. For infection with pseudotype baculoviruses bearing CD46 or SLAM, we transfected target cells with expression plasmids encoding either the hemagglutinin and fusion proteins of the Edmonston strain (EdH and EdF) or those of the Ichinose strain (IcH and IcF) measles viruses. The pCA-EdH, pCA-EdF, pCA-IcH, and pCA-IcF plasmids were kindly provided by K. Takeuchi (63).

**Construction of pseudotype baculoviruses.** The gp64 gene of the AcMNPV-bacmid (bMON14272; Invitrogen) was replaced with the chloramphenicol acetyltransferase (CAT) gene as described previously with slight modifications (5, 33). Briefly, the CAT gene was amplified by PCR with the Chl-Fw-*Spe*I (5′-GGAC TAGTCCGAATAAATACCTGTGACGG-3′) and Chl-Rv-*Bgl*II (5′-GAAG ATCTCGTCAATTATTACCTCCACGG-3′) primers using the pBT plasmid (Stratagene, La Jolla, Calif.) as a template. Following digestion with SpeI and BglII, the amplified CAT gene replaced the gp64 gene of pUCgp64locus to create p64locus/cat. To construct a gp64-null AcMNPV-bacmid, bMONΔ64/cat, the p64locus/cat plasmid was linearized by digestion with NdeI and cotransfected with bMON14272 into Sf9 cells. Forty-eight hours posttransfection, the cells were washed with cold phosphate-buffered saline and lysed in proteinase K buffer (50 mM Tris-HCl [pH 7.4], 100 mM NaCl, 1 mM EDTA, and 0.5% sodium dodecyl sulfate [SDS]). DNA was purified from cell lysates by phenol-chloroform extraction and then transformed into *Escherichia coli* DH10B competent cells (Invitrogen) by electroporation using a Gene Pulser (Bio-Rad, Hercules, Calif.). Resistant colonies were selected in kanamycin and chloramphenicol. Disruption of the gp64 gene was confirmed by PCR in a bMON14272-transformed colony that was resistant to kanamycin and chloramphenicol (Fig. 1A). To generate DH10BacΔ64/cat, we cotransfected bMONΔ64/cat and the helper plasmid pMON7124 into DH10B cells. To construct recombinant bacmids, DH10BacΔ64/cat was transformed with transfer vectors and selected according to the manufacturer's instructions. To separate recombinant bacmids from the pMON7124 helper plasmid, miniprep bacmid DNA was transformed into DH10B cells by electroporation. To generate pseudotype baculoviruses, bacmids lacking the gp64 gene and possessing both an exogenous ligand gene and the luciferase gene under the polyhedrin and CAG promoters, respectively, were transfected into Sf9 cells. Fifteen micrograms of the bacmid DNA was used to transfect $5 \times 10^6$ Sf9 cells in a 10-cm-diameter dish by using 30 μl of UniFector reagent (B-Bridge). Four days after transfection, 500 ml of culture supernatants (50 dishes) was harvested. The resulting pseudotype baculoviruses, AcΔ64/gp64/CAluc, AcΔ64/VSVG/CAluc, AcΔ64/CD46/CAluc, AcΔ64/SLAM/CAluc, and AcΔ64/SLAMcyto7/CAluc, were concentrated ~2,000 times by ultracentrifugation as described previously (66). The number of virus particles was determined from the signal intensity by Western blotting for the capsid protein vp39. Although both AcΔ64/gp64/CAluc and AcΔ64/VSVG/CAluc infected and repli-

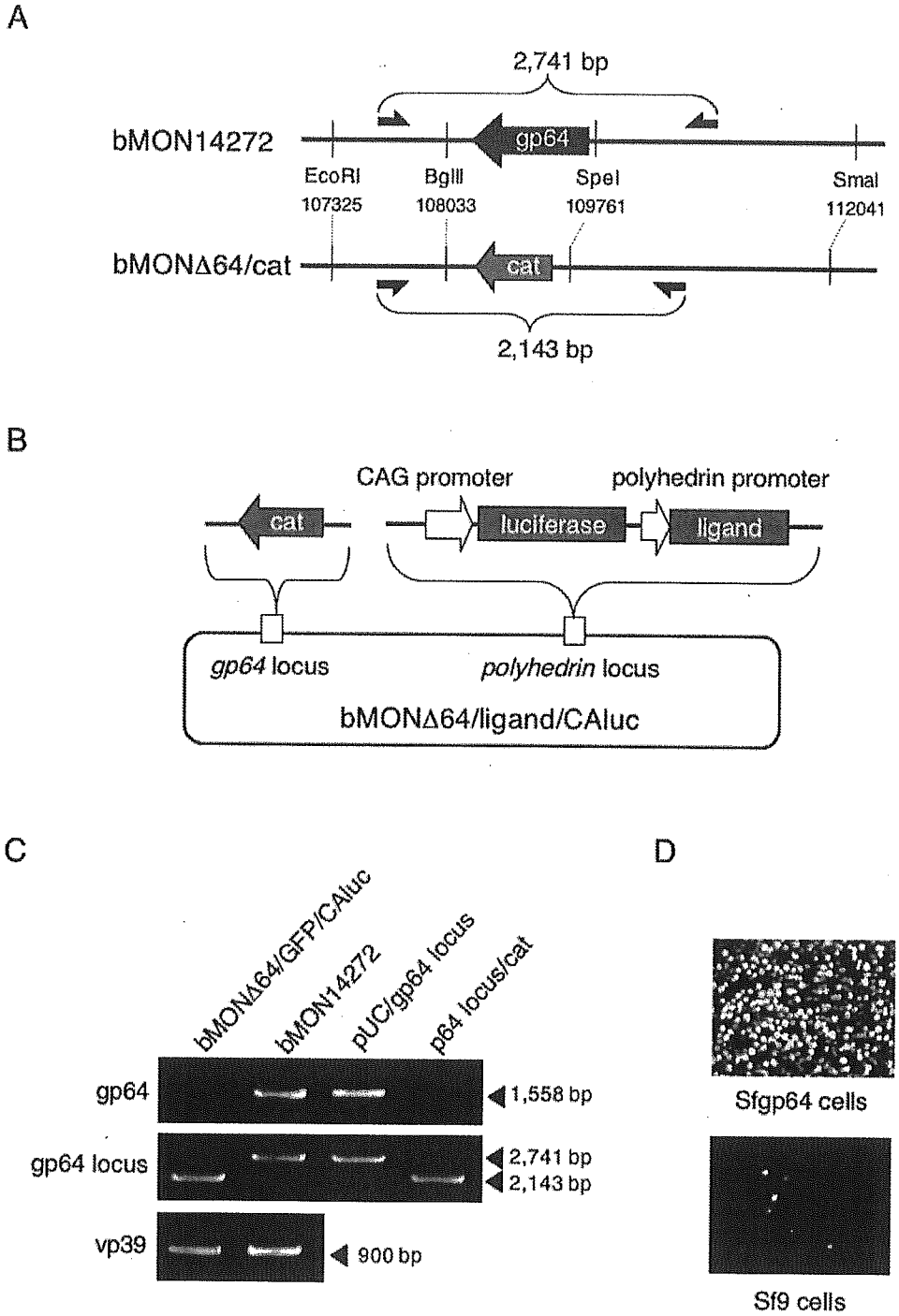


FIG. 1. (A) Schematic representations of the gp64 loci of the AcMNPV (bMON14272) and gp64-null AcMNPV (bMONΔ64/cat) bacmids. The gp64 gene (BglII/SpeI fragment corresponding to 108,033 to 109,761 nt) (3) of bMON14272 was replaced with the CAT gene by homologous recombination. The arrows indicate the locations of the PCR primers within the gp64 loci. (B) Construction of the recombinant bacmid bMONΔ64/ligand/CAluc. The gp64 gene in bMON14272 was replaced with the CAT gene. The desired ligand and luciferase genes were inserted under the control of the polyhedrin and CAG promoters, respectively, within the polyhedrin locus. (C) The bacmids bMONΔ64/ligand/CAluc and bMON14272 and plasmids containing the gp64 locus, pUC/gp64locus, and p64locus/cat (the gp64 locus with the CAT gene replacement) were amplified by PCR using primers specific for gp64, the gp64 locus, and vp39, a nucleocapsid protein of AcMNPV used as an internal control. Primers for gp64 and vp39 amplified fragments of 1,558 and 900 bp, respectively. The gp64 locus primers generated 2,741- and 2,143-bp fragments corresponding to the wild-type gp64 locus and the mutant locus with the CAT gene replacement shown in panel A, respectively. (D) Sfgp64 and Sf9 cells were transfected with bMONΔ64/GFP/CAluc. GFP expression was examined by fluorescence microscopy 4 days posttransfection.

cated in Sf9 cells, it was not possible to determine the infectivity in the cases of the pseudotype baculoviruses possessing ligands incapable of entering into insect cells. To standardize the viral titer, we determined the amount of viral capsid protein vp39 by semiquantitative Western blot analysis. The infectious titer determined by plaque assay in Sf9 cells correlated well with the intensity of the vp39 signal obtained by Western blotting for both AcΔ64/gp64/CAluc and AcΔ64/VSVG/CAluc (data not shown). Pseudotype baculovirus titers are expressed as relative infectious units (RIU) in this study. To confirm the absence of gp64 in the bacmids, we synthesized oligonucleotide primers specific for the gp64 gene, the gp64 locus, and the vp39 gene as follows: for the gp64 gene, gp64-Fw (Bgl) (5′-AAAGATCTACCATGGTAAGCGCTATTGTTT-3′) and gp64-Rv (Sal) (5′-TTGTCGACTTAATATTGTCTATTACGGTTT-3′); for the gp64locus, gp64locus-Fw (5′-GCACGGATTGGGGAGAGGACGGATTTT-3′) and gp64locus-Rv (5′-AGCTCGTTATTCAAGTGTCCCGCGTAC-3′); and for vp39, vp39-Fw (5′-ATATGGCGCTAGTGCCCGTGGGTATGG-3′) and vp39-Rv (5′-GACGGCTATTCCTCCACCTGCTGCCTG-3′). PCR amplification was performed using *Taq* DNA polymerase (Invitrogen) according to the manufacturer's protocol.

**Stability of pseudotype baculoviruses during passage in Sfgp64 cells.** Culture supernatants from Sfgp64 cells transfected with recombinant bacmids were harvested 4 days after transfection. After serial passage in Sfgp64 cells for 4 days, each Sfgp64 cell supernatant was inoculated into Sf9 cells. The culture supernatants were further inoculated into Sf9 cells to examine the generation of replication-competent revertants during the replication in Sfgp64 cells. The presence of replication-competent virus in the culture supernatants was assessed by the appearance of cytopathic effect and GFP expression in Sf9 cells. GFP expression in insect cells was observed by fluorescence microscopy (UFX-II; Nikon, Tokyo, Japan). The generation of replication-competent viruses incorporating gp64 was examined by PCR using the viral DNA as a template. The supernatants of Sfgp64 cells were concentrated by centrifugation at 18,000 × *g* for 45 min at 4°C. Viral DNA, purified from replication-competent revertants by phenol-chloroform extraction, was examined by Southern blot analysis. DNA was digested with BglII or PstI, separated by electrophoresis on a 0.6% agarose gel, and transferred to a Hybond N+ nylon membrane (Amersham Biosciences, Piscataway, N.J.). PCR primers [gp64-Fw (Bgl) and gp64-Rv (Sal) for the gp64 gene or vp39-Fw and vp39-Rv for the vp39 gene] were used to amplify the target fragments for use as hybridization probes. PCR products were purified and labeled using the ECL direct nucleic acid labeling and detection system (Amersham Biosciences) according to the manufacturer's instructions. Fragments containing the gp64 or vp39 gene were visualized using image analyzer LAS-3000 (Fujifilm, Tokyo, Japan).

**Incorporation of ligands into pseudotype particles.** To examine the expression of ligand proteins in insect cells or the incorporation of the ligands into pseudotype particles, cell lysates or purified baculoviruses were separated by SDS-polyacrylamide gel electrophoresis and electroblotted onto Hybond-P polyvinylidene difluoride membranes (Amersham Bioscience). After being blocked in phosphate-buffered saline containing 5% skim milk and 0.05% Tween 20 (Sigma), the membranes were incubated at room temperature for 1 h with a rabbit polyclonal anti-CD46 antibody (H-294; 1:200) (Santa Cruz, Santa Cruz, Calif.) or one of the following mouse monoclonal antibodies: anti-gp64 (AcV5; 1:1,000) (kindly provided by P. Faulkner) (22), anti-VSVG (P5D4; 1:2,000) (Sigma), anti-SLAM (123317; 1:200) (R&D systems, Minneapolis, Minn.), or anti-vp39 (236; 1:2,000) (kindly provided by G. F. Rohrmann) (51). The membranes were then incubated in horseradish peroxidase-conjugated anti-mouse IgG or anti-rabbit IgG antibodies at room temperature for 1 h. Immunoreactive bands were visualized using enhanced-chemiluminescence Super Signal West Femto substrate (Pierce, Rockford, Ill.) (47).

**Reporter gene expression by pseudotype baculoviruses.** AcΔ64/gp64/CAluc and AcΔ64/VSVG/CAluc baculoviruses were inoculated into $3.0 \times 10^4$ 293T and BHK cells. Twenty-four hours after infection, the cells were lysed in Bright-Glo luciferase substrate (Promega, Madison, Wis.) according to the manufacturer's instructions. Relative light units were measured using a luminometer (AB-2200; ATTO Co. Ltd., Tokyo, Japan). To demonstrate ligand-directed gene targeting by AcΔ64/CD46/CAluc, AcΔ64/SLAMCAluc, and AcΔ64/SLAMcyto7/CAluc baculoviruses, $3.0 \times 10^4$ BHK cells were cotransfected with either pCA-EdF and pCA-EdH or pCA-IcF and pCA-IcH and then infected with $5.0 \times 10^6$ RIU of pseudotype baculoviruses at 24 h posttransfection. Luciferase expression was determined after a 24-h incubation.

**Inhibition of gene transduction by specific antibodies against ligands.** To examine ligand-directed gene transduction by pseudotype baculoviruses, we examined the neutralization of gene transduction by antibodies specific for the ligands presented by the pseudotypes. The appropriate dilutions of anti-gp64 (AcV1), anti-VSVG (I1) (kindly provided by M. A. Whitt) (30), anti-CD46 (M75) (Seikagaku Co. Ltd., Tokyo, Japan), or anti-SLAM (IPO-3) (Biodesign International, Saco, Maine) antibodies were preincubated with each virus ($10^6$ RIU) at 37°C for 60 min and then inoculated into the appropriate target cells. After incubation at 37°C for 24 h, we determined the neutralization by the included antibodies from the reduction of luciferase expression.

**Entry of pseudotype baculovirus into target cells.** BHK cells expressing hemagglutinin and fusion proteins derived from the Edmonston strain of measles virus were preincubated with either ammonium chloride (2, 10, or 50 mM) (Wako Pure Chemical Industries, Osaka, Japan) or chloroquine (20, 100, or 500 μM) (Sigma) for 1 h. The cells were then inoculated with $1.0 \times 10^6$ RIU of AcΔ64/CD46/CAluc, AcΔ64/gp64/CAluc, or AcΔ64/VSVG/CAluc in the presence of the above-mentioned reagents. The effects of ammonium choloride and chloroquine on gene transduction by pseudotype baculoviruses were determined by the changes in luciferase expression.

**Electron microscopy.** Viral particles purified by ultracentrifugation as described above were put onto carbon-coated copper 400-mesh electron microscopy grids for 15 min. After being washed in water, the grids were negatively stained with 1% (wt/vol) uranyl acetate and examined using a Hitachi (Tokyo, Japan) H-7100 electron microscope at 75 kV. For immunoelectron microscopy, virus particles put onto grids were incubated with murine monoclonal antibodies specific for VSVG (I1) or CD46 (E4.3) (Santa Cruz) and then treated with a gold particle-conjugated anti-mouse IgG antibody (British Biocell International, Ltd., Cardiff, United Kingdom). Samples were stained and observed as described above.

## RESULTS

**Construction of recombinant AcMNPV lacking the gp64 gene.** The gp64 gene of the AcMNPV bacmid, bMON14272, was replaced with the CAT gene by homologous recombination in Sf9 cells using a modification of the methods reported by Bideshi and Federici (5) and Lung et al. (33) (Fig. 1A). We cotransfected bMON14272 and a linearized p64locus/cat plasmid bearing the CAT gene in place of the gp64 gene into Sf9 cells. DNA, extracted from the cells 48 h after transfection, was then transformed into competent DH10B cells. The disruption of the gp64 gene in colonies selected with kanamycin and chloramphenicol was confirmed by PCR (data not shown). We also constructed a recombinant bacmid, bMONΔ64/GFP/CAluc, which contained the insertion of the GFP gene under the control of the polyhedrin promoter and the luciferase gene under the control of the CAG promoter into the polyhedrin locus of the gp64-null bacmid (Fig. 1B). Disruption of gp64 in bMONΔ64/GFP/CAluc was confirmed by PCR using a series of specific primers (Fig. 1C). PCR with primers specific for the vp39 gene, used as an internal control for the AcMNPV bacmid, amplified a 900-bp product from both the bMONΔ64/GFP/CAluc and parent bMON14272 bacmids. The gp64 gene (1,558 bp) was amplified from bMON14272 and pUC/64locus, but not from bMONΔ64/GFP/CAluc and p64locus/cat. The 2,741- and 2,143-bp fragments corresponding to the wild-type and mutant gp64 genes, respectively, were amplified using gp64 locus-specific primers. The wild-type gene was amplified from bMON14272 and pUC/gp64locus, while the mutant gene was amplified from bMONΔ64/GFP/CAluc and p64locus/cat (Fig. 1A and C). These data indicate that the gp64 gene was replaced with the cat gene in bMONΔ64/GFP/CAluc. Previous studies demonstrated that gp64-null AcMNPV could propagate in $Sf9^{OP64\text{-}6}$ or $Sf9^{Op1D}$ cell lines constitutively expressing the gp64 protein of *Orgyia pseudotsugata* NPV (OpNPV) but not in untransfected Sf9 cells (40, 49). We then established a cell line, Sfgp64, constitutively expressing the gp64 gene derived from AcMNPV. The pAFgp64 plasmid, carrying the gp64 gene of AcMNPV without any flanking sequence, was used to

avoid homologous recombination between the viral genome and the plasmid. To examine the replication competency of gp64-null AcMNPV (AcΔ64/GFP/CAluc), Sfgp64 and Sf9 cells were transfected with bMONΔ64/GFP/CAluc. We assessed the propagation of infectious virus by measuring GFP expression by fluorescence microscopy. Forty-eight hours posttransfection, ~10% of the Sfgp64 and Sf9 cells were GFP positive (data not shown). While Sfgp64 cells exhibited the spread of infection 96 h posttransfection, Sf9 cells did not (Fig. 1D). These data indicate that AcΔ64/GFP/CAluc can replicate only in Sfgp64 cells, not in Sf9 cells.

**Appearance of revertants incorporating the gp64 gene during replication in Sfgp64 cells.** To determine the stability of AcΔ64/GFP/CAluc during replication in Sfgp64 cells, we serially passaged AcΔ64/GFP/CAluc in Sfgp64 cells. Culture supernatants of Sfgp64 cells collected 4 days after transfection with bMONΔ64/GFP/CAluc (passage 1) were inoculated into Sfgp64 cells. The supernatants were further passaged in Sfgp64 cells for 4 days. To examine the appearance of replication-competent viruses, the culture supernatants from each passage were inoculated into Sf9 cells. At 4 days postinfection, we examined GFP expression in Sf9 cells by fluorescence microscopy (Fig. 2A). The expression of GFP was observed in Sf9 cells inoculated with Sfgp64 culture supernatants, irrespective of the passage history. As gp64-negative AcΔ64/GFP/CAluc baculovirus only transiently carries gp64, progeny viruses produced in Sf9 cells should not be infectious. The supernatants of Sf9 cells inoculated with supernatants recovered after >3 passages (passages 3, 4, and 5) with Sfgp64 cells exhibited infectivity to Sf9 cells, suggesting the generation of replication-competent revertants incorporating the gp64 gene into the viral genome. To confirm the incorporation of gp64 into the viral genome, virus particles were purified from the supernatants of each Sfgp64 passage. The presence of the gp64 gene within the viral genome was determined by PCR. We detected the gp64 gene in viruses obtained from the culture supernatants of passages 3, 4, and 5 but not in those from the first and second passages (Fig. 2B). Furthermore, PCR amplification of viral DNA with the gp64 locus-specific primers revealed that a 2,143-bp fragment, corresponding to the mutant form, was detected in the genome of AcΔ64/GFP/CAluc, while a 2,741-bp fragment, corresponding to the wild-type form, was amplified from Ac14272, irrespective of the number of passages. These results confirmed that the emergence of replication-competent virus during the passage in Sfgp64 cells is not due to the contamination of the parental virus, Ac14272. The recombinant virus incorporated the gp64 gene into the AcΔ64/GFP/CAluc genome during propagation in Sfgp64 cells.

Plasmid DNA can be integrated into multiple sites within the viral genome by nonhomologous recombination upon cotransfection of plasmid DNA with the baculovirus genome in Sf9 cells (71). To determine if gp64 genes integrated into the baculovirus genome by nonhomologous recombination during propagation in Sfgp64 cells, we analyzed the DNAs of three independent revertant viruses by PCR and Southern blot analyses. Viral DNA was extracted from these revertant viruses and analyzed by PCR as described above (Fig. 3A). We detected the gp64 gene in all revertant viruses and bMON14272 but not in the parental bacmid, bMONΔ64/GFP/CAluc. The gp64 locus primers amplified the mutant 2,143-bp fragment from all revertant viruses and the parental bMONΔ64/GFP/CAluc bacmid, not the 2,741-bp wild-type fragment that could be amplified from bMON14272. These results confirmed that the three independent revertant viruses, instead of deriving from contaminating wild-type virus, had incorporated the gp64 gene into their genomes exogenously. DNA from the revertants was digested with BglII or PstI, which do not digest sequences within the gp64 or vp39 genes, and hybridized to gp64- or vp39-specific probes (Fig. 3B). If the gp64 gene integrated into the viral genome by nonhomologous recombination, the digested fragments containing the gp64 gene would be of different sizes. Following digestion with BglII, the DNA fragments containing the gp64 gene in the revertants differed in size from each other (Fig. 3B, lanes 3 to 5). When digested with PstI, the sizes of the fragments containing the gp64 gene were similar in revertant clones 2 and 3 (Fig. 3B, lanes 9 to 10), indicating that the gp64 gene may have integrated into nearby sites in the viral genomes of clones 2 and 3. The fragment containing the gp64 gene in revertant clone 1 following digestion with either BglII or PstI was similar to that seen in bMON14272 (Fig. 3B lanes 3 and 8). These results, however, were not due to contamination with bMON14272, as the PCR analysis demonstrated that the gp64 locus of revertant clone 1 was of the mutant type (Fig. 3A). These data suggested that the gp64 gene integrated into the virus genomes of the revertants by nonhomologous recombination. As an internal control, the vp39 gene was detected in fragments of the predicted sizes (31,975 bp when digested with BglII and 29,009 bp when digested with PstI) in all viruses. To determine the sites of integration of the gp64 gene in the genomes of the revertants, we tried to sequence from within the gp64 gene out into the baculovirus genome by using an internal gp64 primer. In revertant 2, the sequences including the actin promoter and the gp64 gene were detected upstream of the polyhedrin promoter, where no homologous sequence was observed. In revertants 1 and 3, however, sequence analyses by the internal primer obtained only sequences of pAFgp64 and could not reach the integration site, due to a large insertion of the plasmid sequence (data not shown).

**Characterization of pseudotype baculovirus carrying VSVG.** Previous studies demonstrated that the gp64 protein plays a critical role in infection of various mammalian cells, as well as insect cells (66). To determine if the pseudotype baculoviruses bearing foreign viral envelope proteins in place of gp64 can infect and express foreign genes within mammalian cells, we constructed a gp64-null pseudotype virus, AcΔ64/VSVG/CAluc, by the transfection of bMONΔ64/VSVG/CAluc, which encodes the VSVG gene under the control of the polyhedrin promoter and the luciferase gene under the control of the CAG promoter, into Sf9 cells (Fig. 1B). As a control, we also generated AcΔ64/gp64/CAluc, in which the gp64 gene under the control of the polyhedrin promoter replaced the VSVG gene in the above-mentioned virus. Sf9 cells were transfected with appropriate bacmids and incubated for 4 days. The pseudotype baculoviruses in the culture supernatants were concentrated and purified by ultracentrifugation ($10^8$ to $10^9$ RIU/ml). To examine the expression and incorporation of the glycoproteins into virions, we transfected these bacmid constructs into Sf9 cells. The cell lysates and the purified virus particles were examined by Western blot analysis (Fig. 4A). VSVG and gp64

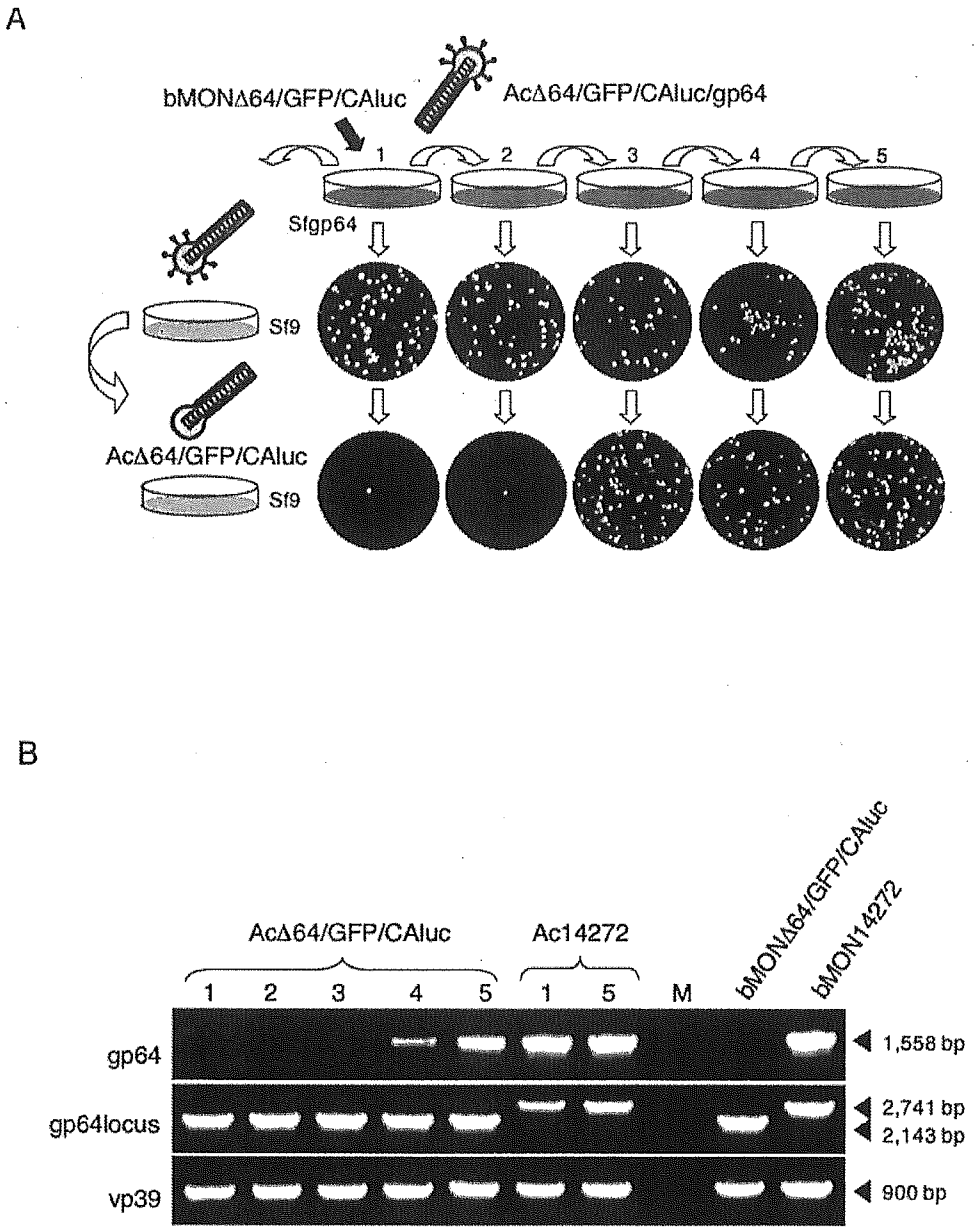


FIG. 2. Appearance of replication-competent viruses incorporating the gp64 gene during passage in Sfgp64 cells. (A) Sfgp64 cells were transfected with bMONΔ64/GFP/CAluc. Culture supernatants were harvested 4 days after transfection and then serially passaged in Sfgp64 cells at 4-day intervals. Each culture supernatant from Sfgp64 cells was passaged two more times in Sf9 cells to detect the appearance of replication-competent viruses. GFP expression in Sf9 cells was examined by fluorescence microscopy 4 days after infection. (B) PCR analysis of purified virus particles from the supernatant of each Sfgp64 cell passage. The gp64 gene was detectable in particles obtained from the third or later passages. The numbers above the lanes represent the passage numbers. The bMONΔ64/GFP/CAluc and bMON14272 bacmids and Ac14272, generated from bMON14272 and passaged in Sfgp64 cells, were used as controls. M is the culture supernatant of uninfected Sfgp64 cells concentrated under the same conditions as the virus particles. The primers amplified fragments as detailed in the legend to Fig. 1.

were expressed in the cells transfected with the appropriate bacmids. The proteins were also detected in the purified AcΔ64/VSVG/CAluc and AcΔ64/gp64/CAluc viruses, respectively, but not in AcΔ64/GFP/CAluc.

To assess the efficacy of mammalian cell gene transduction by the pseudotype baculoviruses, 293T and BHK cells were inoculated with various amounts of pseudotype viruses (Fig. 4B). Similar levels of reporter gene expression were observed in a dose-dependent manner in both cell lines following infection with AcΔ64/gp64/CAluc and AcΔ64/VSVG/CAluc. AcΔ64/GFP/CAluc, however, was unable to infect either cell line. To confirm the role of gp64- or VSVG-mediated gene transduction into mammalian cells by the pseudotype baculoviruses, we attempted to neutralize 293T cell infection using

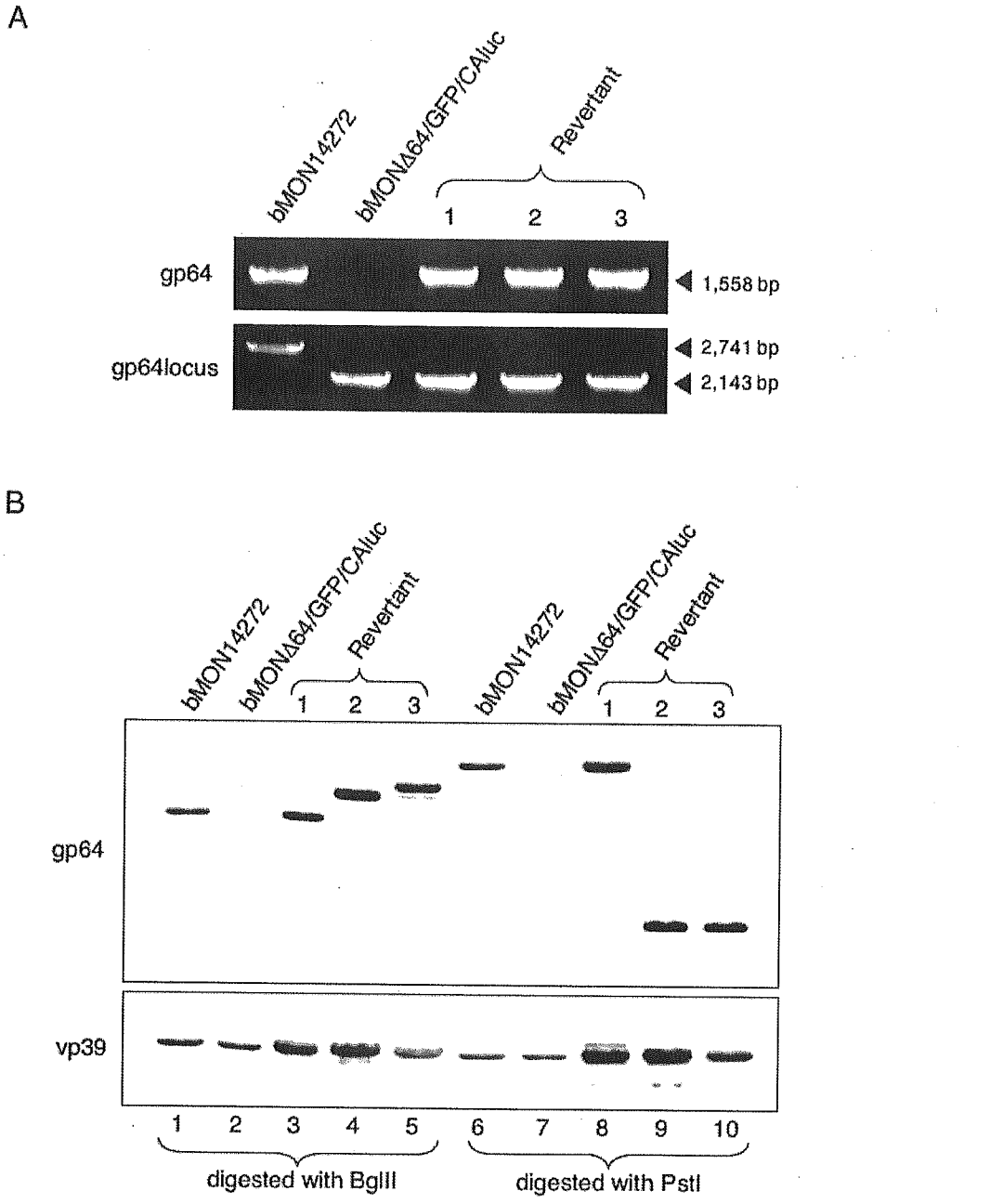


FIG. 3. Incorporation of the gp64 gene into gp64-null baculovirus genomes by nonhomologous recombination. (A) PCR analysis of three independent revertant viruses. In each revertant virus, the gp64 gene and gp64 locus primer pairs produced 1,558- and 2,143-bp fragments, respectively, indicating the presence of the mutant gp64 locus. (B) Southern blot analysis of revertant viruses. Viral DNA was digested with BglII or PstI, separated, and hybridized to gp64- or vp39-specific probes. Fragments containing the gp64 gene were detectable in all of the revertant viruses, but the fragment sizes differed. The vp39 gene, used as an internal control, was detectable in all revertant DNAs and bacmids. The numbers above the lanes represent the revertant clones. The bMONΔ64/GFP/CAluc and bMON14272 bacmids were used as controls.

specific monoclonal antibodies against gp64 and VSVG. Luciferase expression in 293T cells infected with either AcΔ64/gp64/CAluc or AcΔ64/VSVG/CAluc was specifically inhibited by antibodies against gp64 or VSVG, respectively (Fig. 4C). These results indicate that reporter gene expression in mammalian cells inoculated with pseudotype baculoviruses relies on the interactions mediated by the ligand proteins on the viral particles.

**Ligand-directed gene targeting by pseudotype baculovirus.** To demonstrate the ligand-directed gene transduction of target cells by pseudotype baculoviruses, we constructed pseudotype viruses bearing CD46 or SLAM in place of the gp64

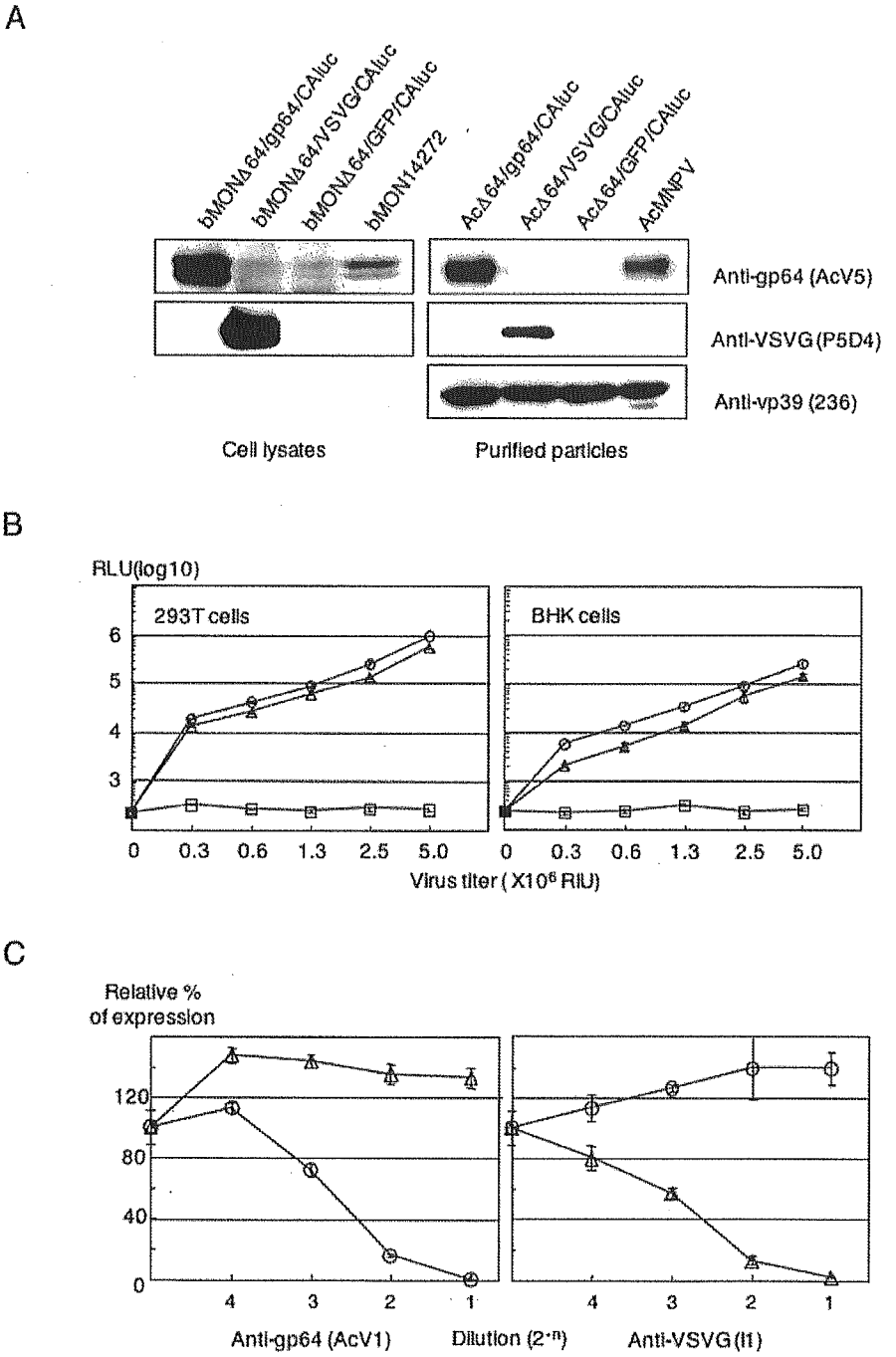


FIG. 4. Characterization of pseudotype baculoviruses bearing VSVG. (A) VSVG and gp64 expression in Sf9 cells transfected with the bMONΔ64/gp64/CAluc, bMONΔ64/VSVG/CAluc, bMONΔ64/GFP/CAluc, or bMON14272 bacmid were examined by Western blot analysis using monoclonal antibodies specific for VSVG (P5D4) and gp64 (AcV5) (left). The incorporation of gp64 and VSVG into pseudotype particles, AcΔ64/gp64/CAluc, AcΔ64/VSVG/CAluc, AcΔ64/GFP/CAluc, or AcMNPV, was examined by Western blot analysis using monoclonal antibodies specific for gp64, VSVG, and vp39 (236) (right). (B) Gene transduction into mammalian cells by pseudotype baculoviruses. 293T or BHK cells ($3 \times 10^4$) were inoculated with various amounts of AcΔ64/gp64/CAluc, AcΔ64/VSVG/CAluc, or AcΔ64/GFP/CAluc. The pseudotype titers are expressed as RIU. Luciferase expression was determined 24 h after infection. The results shown are the means of three independent assays, while the error bars represent the standard deviations. RLU, relative light units. (C) Neutralization of gene transduction into mammalian cells by pseudotype baculoviruses by antibodies specific for the particle ligands. AcΔ64/gp64/CAluc or AcΔ64/VSVG/CAluc ($10^6$ RIU) was preincubated with the indicated dilutions of monoclonal antibodies specific for gp64 (AcV1) or VSVG (I1), respectively, for 60 min at 37°C. Residual activity, determined as luciferase expression in 293T cells 24 h postinfection, is expressed as the relative percentages of expression. The results shown are the means of three independent assays, with the error bars representing the standard deviations.